Leibniz Universität Hannover

Systematic analysis of atom interferometric measurements in complex gravitational environments

Michael Werner
Theory of Quantum Sensing
Leibniz University Hannover

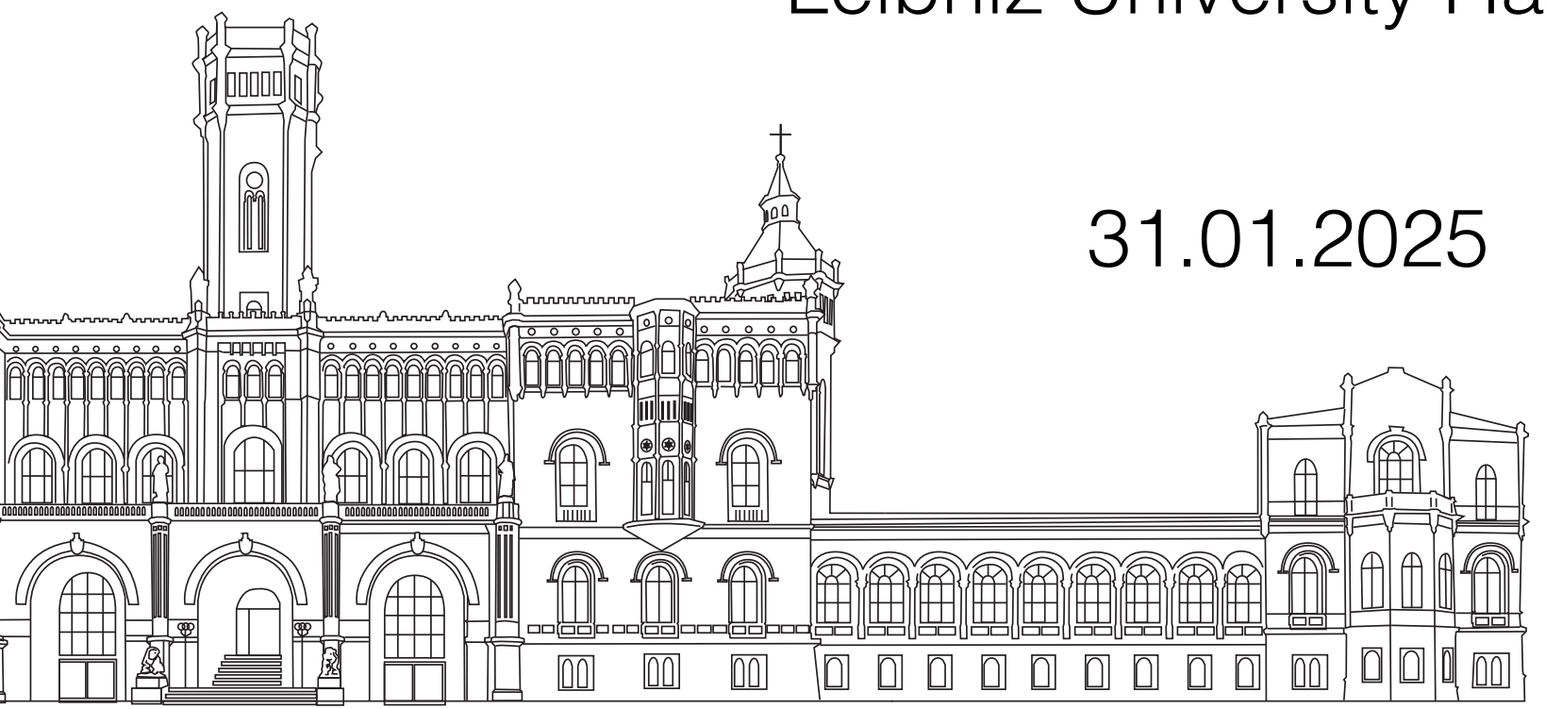

31.01.2025

1. Motivation

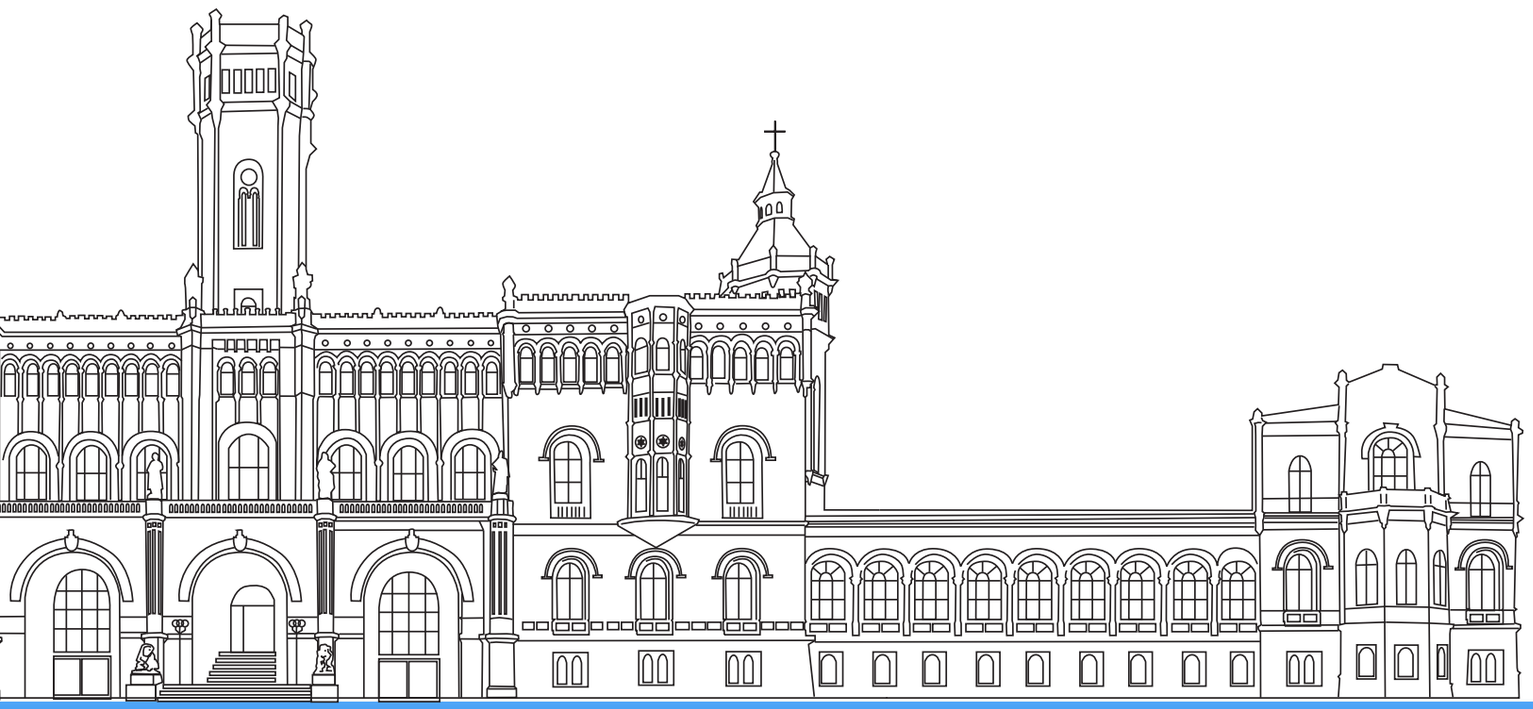

How it started…

Theory colleagues working on general relativity (GR) developed this:

Post-Newtonian Hamiltonian description of an atom in a weak gravitational field

Philip K. Schwartz[1,a] and Domenico Giulini[1,2,b]

[1] *Institute for Theoretical Physics, Leibniz University Hannover, Appelstraße 2, 30167 Hannover, Germany*
[2] *Center of Applied Space Technology and Microgravity, University of Bremen, Am Fallturm 1, 28359 Bremen, Germany*
[a] philip.schwartz@itp.uni-hannover.de
[b] giulini@itp.uni-hannover.de

We wanted to apply this novel GR-Hamiltonian to atom interferometers (AIFs)!

See Schwartz und Giulini, *Post-Newtonian Hamiltonian description of an atom* (2019)

How it started…

Minkowski space

$$g_{\mu\nu} = \eta_{\mu\nu} = \begin{pmatrix} -1 & 0 \\ 0 & \mathbb{1} \end{pmatrix}$$

$\phi =$ Gravitational potential

Newtonian spacetime

$$g_{\mu\nu} = \begin{pmatrix} -1 - 2\frac{\phi}{c^2} & 0 \\ 0 & \mathbb{1} \end{pmatrix}$$

(Parametrized) Post-Newtonian (PPN) spacetime

$$g_{\mu\nu} = \begin{pmatrix} -1 - 2\frac{\phi}{c^2} - 2\beta\frac{\phi^2}{c^4} & 0 \\ 0 & \left(1 - 2\gamma\frac{\phi}{c^2}\right)\mathbb{1} \end{pmatrix}$$

PPN parameters

in GR: $\beta = \gamma = 1$

How it started…

$$H_{\mathrm{C,final}} = \frac{\mathbf{P}^2}{2M}\left[1 - \frac{1}{Mc^2}\left(\frac{\mathbf{p_r}^2}{2\mu} + \frac{e_1 e_2}{4\pi\varepsilon_0 r}\right)\right] + \left[M + \frac{1}{c^2}\left(\frac{\mathbf{p_r}^2}{2\mu} + \frac{e_1 e_2}{4\pi\varepsilon_0 r}\right)\right]\phi(\mathbf{R})$$
$$- \frac{\mathbf{P}^4}{8M^3c^2} + \frac{2\gamma+1}{2Mc^2}\mathbf{P}\cdot\phi(\mathbf{R})\mathbf{P} + (2\beta-1)\frac{M\phi(\mathbf{R})^2}{2c^2}\ ,$$

Center of mass (COM)

Look @ elastic scattering processes (first)
—> Populate the excited state only virtually.

Internal dynamics

$$H_{\mathrm{AL,final}} = -\mathbf{d}\cdot\mathbf{E}^{\perp}_{\mathrm{coord.}}(\mathbf{R}) + \frac{1}{2M}\{\mathbf{P}\cdot[\mathbf{d}\times\mathbf{B}_{\mathrm{coord.}}(\mathbf{R})] + \mathrm{H.c.}\}$$
$$- \frac{m_1 - m_2}{4m_1 m_2}\{\mathbf{p_r}\cdot[\mathbf{d}\times\mathbf{B}_{\mathrm{coord.}}(\mathbf{R})] + \mathrm{H.c.}\}$$
$$+ \frac{1}{8\mu}(\mathbf{d}\times\mathbf{B}_{\mathrm{coord.}}(\mathbf{R}))^2 + \frac{1}{2\varepsilon_0}\int \mathrm{d}^3\mathbf{x}\left(1 + (\gamma+1)\frac{\phi}{c^2}\right)\boldsymbol{\mathcal{P}}_d^{\perp\,2}(\mathbf{x},t)\ ,$$

Atom-Light-Interaction

Treat light fields classical
—> Maxwell’s equations

Light field

Motivation

- Special relativistic effects have been included for multiple AIF geometries.

- How does gravity enter into this description?

- Which GR effects are the most relevant?

- How can we calculate those phase shifts **accurately and swiftly**?

SCIENCE ADVANCES | RESEARCH ARTICLE

PHYSICS

Interference of clocks: A quantum twin paradox

Sina Loriani[1]*, Alexander Friedrich[2]*†, Christian Ufrecht[2], Fabio Di Pumpo[2], Stephan Kleinert[2], Sven Abend[1], Naceur Gaaloul[1], Christian Meiners[1], Christian Schubert[1], Dorothee Tell[1], Étienne Wodey[1], Magdalena Zych[3], Wolfgang Ertmer[1], Albert Roura[2], Dennis Schlippert[1], Wolfgang P. Schleich[2,4,5], Ernst M. Rasel[1], Enno Giese[2]

The phase of matter waves depends on proper time and is therefore susceptible to special-relativistic (kinematic) and gravitational (redshift) time dilation. Hence, it is conceivable that atom interferometers measure general-relativistic time-dilation effects. In contrast to this intuition, we show that (i) closed light-pulse interferometers without clock transitions during the pulse sequence are not sensitive to gravitational time dilation in a linear potential. (ii) They can constitute a quantum version of the special-relativistic twin paradox. (iii) Our proposed experimental geometry for a quantum-clock interferometer isolates this effect.

INTRODUCTION

Proper time is operationally defined (*1*) as the quantity measured by an ideal clock (*2*) moving through spacetime. As the passage of time itself is relative, the comparison of two clocks that traveled along different world lines gives rise to the twin paradox (*3*). Whereas this key feature of relativity relies on clocks localized on world lines, today's clocks are based on atoms that can be in a superposition of different trajectories. This nature of quantum objects is exploited by matter-wave interferometers, which create superpositions at macroscopic spatial separations (*4*). One can therefore envision a single quantum clock such as a two-level atom in a superposition of two different world lines, suggesting a twin paradox, in principle susceptible to any form of time dilation (*5*–*7*). We demonstrate which atom interferometers implement a quantum twin paradox, how quantum clocks interfere, and their sensitivity to different types of time dilation.

The astonishing consequences of time dilation can be illustrated by the story of two twins (*3*), depicted in Fig. 1A: Initially at the same position, one of them decides to go on a journey through space and leaves his brother behind. Because of their relative motion, he experiences time dilation and, upon meeting his twin again after the voyage, has aged slower than his brother who remained at the same position. Although this difference in age is notable by itself, the twin who traveled could argue that, from his perspective, his brother has moved away and returned, making the same argument. This twin paradox can be resolved in the context of relativity, where it becomes apparent that not both twins are in an inertial system for the whole duration. In the presence of gravity, two twins that separate and reunite experience additional time dilation depending on the gravitational potential during their travel. The experimental verifications of the effect that leads to the difference in age, namely, special-relativistic and gravitational time dilation, were milestones in the development of modern physics and have, for instance, been performed by the comparison of two atomic clocks (*8*–*10*). Atomic clocks, as used in these experiments, are based on microwave and optical transitions between electronic states and define the state of the art in time keeping (*11*).

In analogy to optical interferometry, atom interferometers measure the relative phase of a matter wave accumulated during the propagation by interfering different modes. Although it is possible to generate these interferometers through different techniques, we focus here on light-pulse atom interferometers like the one of Kasevich and Chu (*12*) with two distinct spatially separated branches, where the matter waves are manipulated through absorption and emission of photons that induce a recoil to the atom. Conventionally, these interferometers consist of a series of light pulses that coherently drive atoms into a superposition of motional states, leading to the spatial separation. The branches are then redirected and finally recombined such that the probability to find atoms in a specific momentum state displays an interference pattern and depends on the phase difference $\Delta\varphi$ accumulated between the branches that is susceptible to inertial forces. Hence, light-pulse atom interferometers do not only provide high-precision inertial sensors (*13*, *14*) with applications in tests of the foundations of physics (*15*–*21*) but also constitute a powerful technique to manipulate atoms and generate spatial superpositions.

Atom interferometry, in conjunction with atomic clocks, has led to the idea of using time dilation between two branches of an atom interferometer as a which-way marker to measure effects like the gravitational redshift through the visibility of the interference signal (*5*, *6*). However, no specific geometry for an atom interferometer was proposed and no physical process for the manipulation of the matter waves was discussed. The geometry as well as the protocols used for coherent manipulation crucially determine whether and how the interferometer phase depends on proper time (*22*). Therefore, the question of whether the effects connected to time dilation can be observed in light-pulse atom interferometers is still missing a conclusive answer.

In this work, we study a quantum version of the twin paradox, where a single twin is in a superposition of two different world lines, aging simultaneously at different rates, illustrated in Fig. 1B. We show that light-pulse atom interferometers can implement the scenario where time dilation is due to special-relativistic effects but are insensitive to gravitational time dilation. To this end, we establish a relation between special-relativistic time dilation and kinematic asymmetry of closed atom interferometers, taking the form of recoil measurements (*15*, *21*, *23*, *24*). For these geometries, a single atomic clock in a superposition of two different trajectories undergoes special-relativistic time

[1]Institut für Quantenoptik, Leibniz Universität Hannover, Welfengarten 1, D-30167 Hannover, Germany. [2]Institut für Quantenphysik and Center for Integrated Quantum Science and Technology (IQST), Universität Ulm, Albert-Einstein-Allee 11, D-89069 Ulm, Germany. [3]Centre for Engineered Quantum Systems, School of Mathematics and Physics, The University of Queensland, St Lucia, QLD 4072, Australia. [4]Hagler Institute for Advanced Study and Department of Physics and Astronomy, Institute for Quantum Science and Engineering (IQSE), Texas A&M AgriLife Research, Texas A&M University, College Station, TX 77843-4242, USA. [5]Institute of Quantum Technologies, German Aerospace Center (DLR), D-89069 Ulm, Germany.
*These authors contributed equally to this work.
†Corresponding author. Email: alexander.friedrich@uni-ulm.de

Idealized gravitational potential

We expand the gravitational potential in a Taylor series:

$$\phi(R_\oplus + z) = \phi_0 + gz - \frac{1}{2}\Gamma_0 z^2 + \frac{1}{3}\Lambda_0 z^3 + \mathcal{O}(z^4)$$

Constant offset $\phi_0 = -\dfrac{GM_\oplus}{R_\oplus}$

Linear gravitational acceleration $g = \dfrac{GM_\oplus}{R_\oplus^2}$

Gravity gradient $\Gamma_0 = \dfrac{GM_\oplus}{R_\oplus^3}$

Second gravity gradient $\Lambda_0 = \dfrac{GM_\oplus}{R_\oplus^4}$

COM Hamiltonian: Propagation Phase

We follow a semiclassical approach with

$$L(z,\dot{z}) = \boxed{-mc^2} + \boxed{\frac{m\dot{z}^2}{2} - m\phi(z)} + \boxed{\frac{1}{mc^2}\left[\frac{m^2\dot{z}^4}{8} - \frac{2\beta-1}{2}m^2\phi(z)^2 - \frac{2\gamma+1}{2}m\phi(z)\dot{z}^2\right]}$$

The phase of an atom then evolves freely as

$$\Delta\Phi_{A\to B} = \frac{1}{\hbar}\int_{t_a}^{t_b} \mathrm{d}t\, L(z_{A\to B}(t), \dot{z}_{A\to B}(t))$$

where the atomic trajectory solves the Euler-Lagrange equation

$$\frac{\mathrm{d}}{\mathrm{d}t}\frac{\partial L}{\partial \dot{z}} - \frac{\partial L}{\partial z} = 0$$

Bound. conditions

$A = (t_a, z_a)$

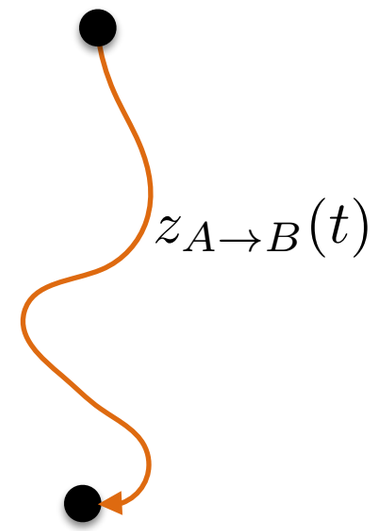

$B = (t_b, z_b)$

Atom-Light Hamiltonian: Bragg scattering

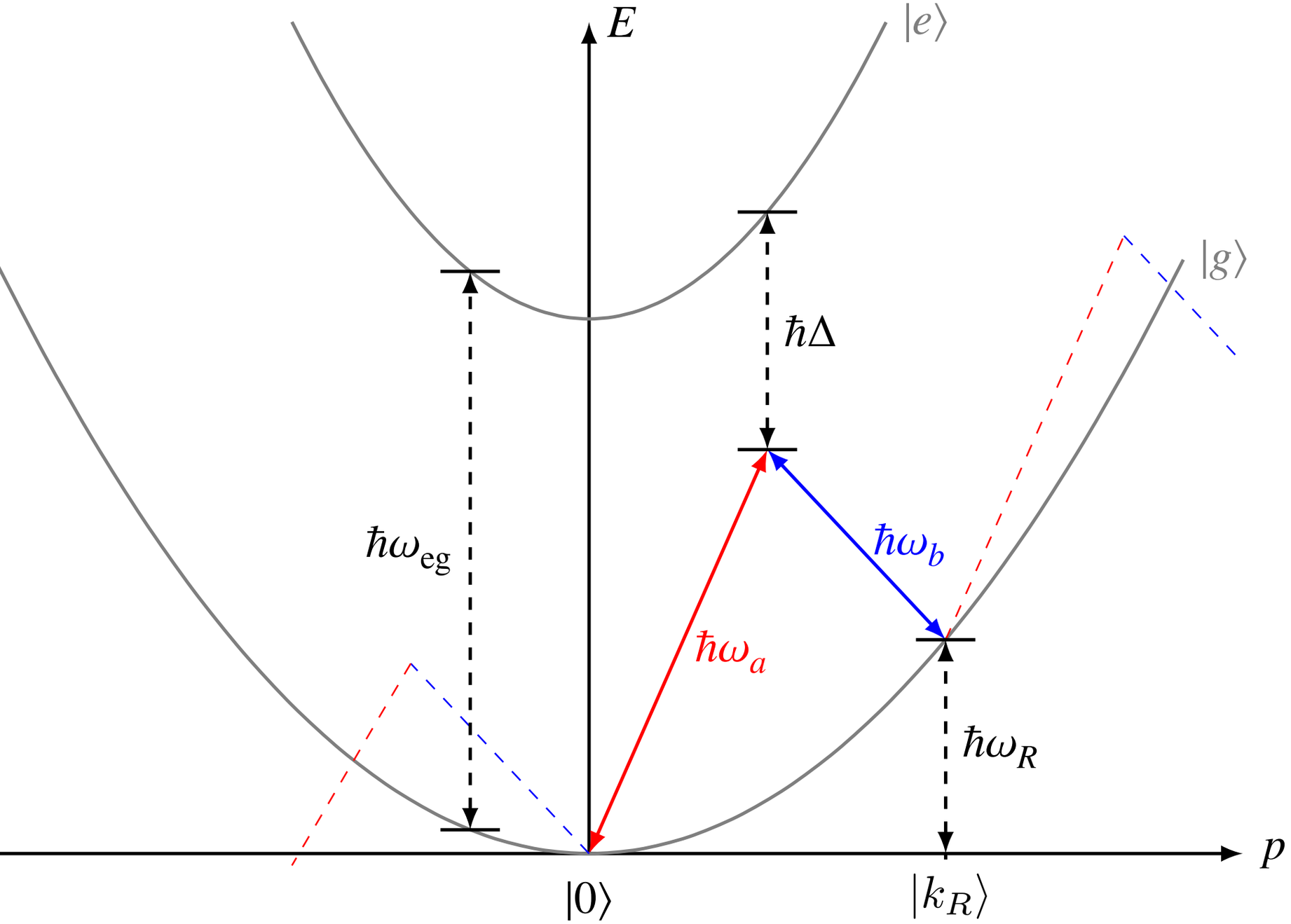

Effective recoil momentum

$$k_R = k_a + k_b$$

Effective recoil frequency

$$\omega_R = \omega_a - \omega_b$$

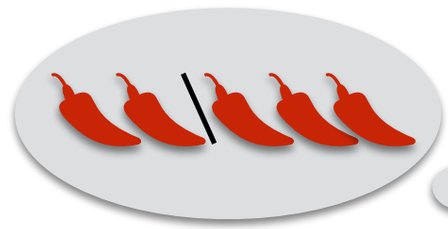

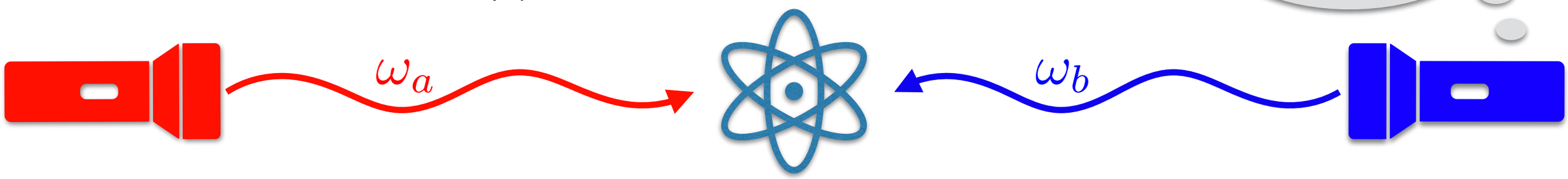

Light Hamiltonian: Maxwell's equations

We analyse Maxwell's equations in vacuum:

$$F_{\alpha\beta}{}^{;\beta} = \nabla^{\beta} F_{\alpha\beta} = \nabla^{\beta}\left(\nabla_{\alpha} A_{\beta} - \nabla_{\beta} A_{\alpha}\right) = 0$$

Three different choices for gauges:

$$\nabla_{\beta} A^{\beta} = A^{\beta}{}_{;\beta} = A_{\beta}{}^{;\beta} = 0,$$

Lorenz gauge

$$\nabla^{i} A_{i} = A_{i}{}^{;i} = 0,$$

Geometric Coulomb gauge

$$\partial^{i} A_{i} = A_{i}{}^{,i} = 0.$$

Background Coulomb gauge

Maxwell's equations: Geometric Coulomb gauge

Writing them out and using the gauge condition:

$$
\begin{aligned}
0 = F_{\nu\mu}{}^{;\mu} &= A_{\mu}{}^{;\mu}{}_{;\nu} - A_{\nu;\mu}{}^{;\mu} \\
&= g^{\mu\lambda}\partial_\lambda\partial_\mu A_\nu - \partial_\nu\partial^\mu A_\mu - g^{\mu\lambda}\Gamma^\sigma{}_{\lambda\mu}(\partial_\sigma A_\nu + \partial_\nu A_\sigma) - g^{\mu\lambda}\Gamma^\sigma{}_{\lambda\nu}\left(\partial_\mu A_\sigma - \partial_\sigma A_\mu\right) \\
&= g^{\mu\lambda}\partial_\lambda\partial_\mu A_\nu - \partial_\nu\partial^0 A_0 - \partial_\nu\partial^i A_i - g^{\mu\lambda}\Gamma^\sigma{}_{\lambda\mu}\partial_\sigma A_\nu + \partial_\nu g^{0\lambda}\Gamma^\sigma{}_{\lambda 0}A_\sigma + \partial_\nu g^{i\lambda}\Gamma^\sigma{}_{\lambda i}A_\sigma \\
&\quad - \left(\partial_\nu g^{\mu\lambda}\right)\Gamma^\sigma{}_{\lambda\mu}A_\sigma - g^{\mu\lambda}\left(\partial_\nu\Gamma^\sigma{}_{\lambda\mu}\right)A_\sigma - g^{\mu\lambda}\Gamma^\sigma{}_{\lambda\nu}\partial_\mu A_\sigma + g^{\mu\lambda}\Gamma^\sigma{}_{\lambda\nu}\partial_\sigma A_\mu \\
&= g^{\mu\lambda}\left(\partial_\lambda\partial_\mu A_\nu - \Gamma^\sigma{}_{\lambda\mu}\partial_\sigma A_\nu - \left(\partial_\nu\Gamma^\sigma{}_{\lambda\mu}\right)A_\sigma - \Gamma^\sigma{}_{\lambda\nu}\partial_\mu A_\sigma + \Gamma^\sigma{}_{\lambda\nu}\partial_\sigma A_\mu\right) \\
&\quad - \partial_\nu\left(\partial^0 A_0 - g^{0\lambda}\Gamma^\sigma{}_{\lambda 0}A_\sigma\right) - \left(\partial_\nu g^{\mu\lambda}\right)\Gamma^\sigma{}_{\lambda\mu}A_\sigma - \partial_\nu\left(\partial^i A_i - g^{i\lambda}\Gamma^\sigma{}_{\lambda i}A_\sigma\right) \\
&= g^{00}\left(\partial_0^2 A_\nu - \Gamma^\sigma{}_{00}\partial_\sigma A_\nu - (\partial_\nu\Gamma^\sigma{}_{00})A_\sigma - \Gamma^\sigma{}_{0\nu}\partial_0 A_\sigma + \Gamma^\sigma{}_{0\nu}\partial_\sigma A_0\right) \\
&\quad - \partial_\nu\left(\partial^0 A_0 - g^{00}\Gamma^\sigma{}_{00}A_\sigma\right) - \left(\partial_\nu g^{00}\right)\Gamma^\sigma{}_{00}A_\sigma - \left(\partial_\nu g^{ij}\right)\Gamma^\sigma{}_{ij}A_\sigma \\
&\quad + g^{ij}\left(\partial_i\partial_j A_\nu - \Gamma^\sigma{}_{ij}\partial_\sigma A_\nu - \left(\partial_\nu\Gamma^\sigma{}_{ij}\right)A_\sigma - \Gamma^\sigma{}_{j\nu}\partial_i A_\sigma + \Gamma^\sigma{}_{j\nu}\partial_\sigma A_i\right).
\end{aligned}
$$

Maxwell's equations: Geometric optics approximation

Ansatz with $\epsilon \ll 1$ of the following form:

$$A_\mu = \left(a_\mu + \epsilon b_\mu + \epsilon^2 c_\mu + \mathcal{O}(\epsilon^3)\right) e^{i\Phi/\epsilon}$$

Amplitudes

$$a_\mu, b_\mu, c_\mu : \mathcal{M} \longrightarrow \mathbb{C}$$

Phase

$$\Phi : \mathcal{M} \longrightarrow \mathbb{R}$$

$$k_\mu = \nabla_\mu \Phi = \partial_\mu \Phi$$

Maxwell's equations: Leading order

$$\mathcal{O}(\epsilon^{-2}): \quad k_\mu k^\mu a_\nu = 0$$

To leading order, geometric optics ensures that the wave vector is **light like.**

$$k_\mu k^\mu = 0$$

$$k_z^2(z) = \left(1 - 2(\gamma+1)\frac{\overline{\phi}(z)}{c^2} + \mathcal{O}(c^{-4})\right) k_0^2(z)$$

$$k_z(z) = \pm\left(1 - (\gamma+1)\frac{\overline{\phi}(z)}{c^2} + \mathcal{O}(c^{-4})\right) k_0(z)$$

Using some more algebra we also find that $k_0(z) = k_0$

Maxwell's equations: Sub-Leading order

Next order equations: $\mathcal{O}(\epsilon^{-1})$

$$(\boldsymbol{\nabla} a_x)\cdot\boldsymbol{k}+\frac{1}{2}a_x\boldsymbol{\nabla}\cdot\boldsymbol{k}=\frac{2\gamma+1}{2c^2}(\partial_z\overline{\phi})k_x a_z-\frac{\gamma+1}{2c^2}(\partial_z\overline{\phi})k_z a_x+\mathcal{O}(\epsilon^0,c^{-4}),$$

$$(\boldsymbol{\nabla} a_y)\cdot\boldsymbol{k}+\frac{1}{2}a_y\boldsymbol{\nabla}\cdot\boldsymbol{k}=\frac{2\gamma+1}{2c^2}(\partial_z\overline{\phi})k_y a_z-\frac{\gamma+1}{2c^2}(\partial_z\overline{\phi})k_z a_y+\mathcal{O}(\epsilon^0,c^{-4}),$$

$$(\boldsymbol{\nabla} a_z)\cdot\boldsymbol{k}+\frac{1}{2}a_z\boldsymbol{\nabla}\cdot\boldsymbol{k}=\frac{\gamma}{2c^2}(\partial_z\overline{\phi})k_z a_z+\mathcal{O}(\epsilon^0,c^{-4}).$$

No corrections to the amplitudes to relevant order.

$$(A_i)=\boldsymbol{A}=\boldsymbol{\mathcal{A}}\,e^{\mathrm{i}\left(k_0 ct\pm\left(1-\frac{\gamma+1}{2}\frac{gz}{c^2}\right)k_0 z\right)}+\boldsymbol{\mathcal{O}}(\Gamma\,c^{-2})\quad\text{with}\quad\boldsymbol{\mathcal{A}}=\begin{pmatrix}A_x\\A_y\\0\end{pmatrix}$$

2. Systematic analysis of AIF classes

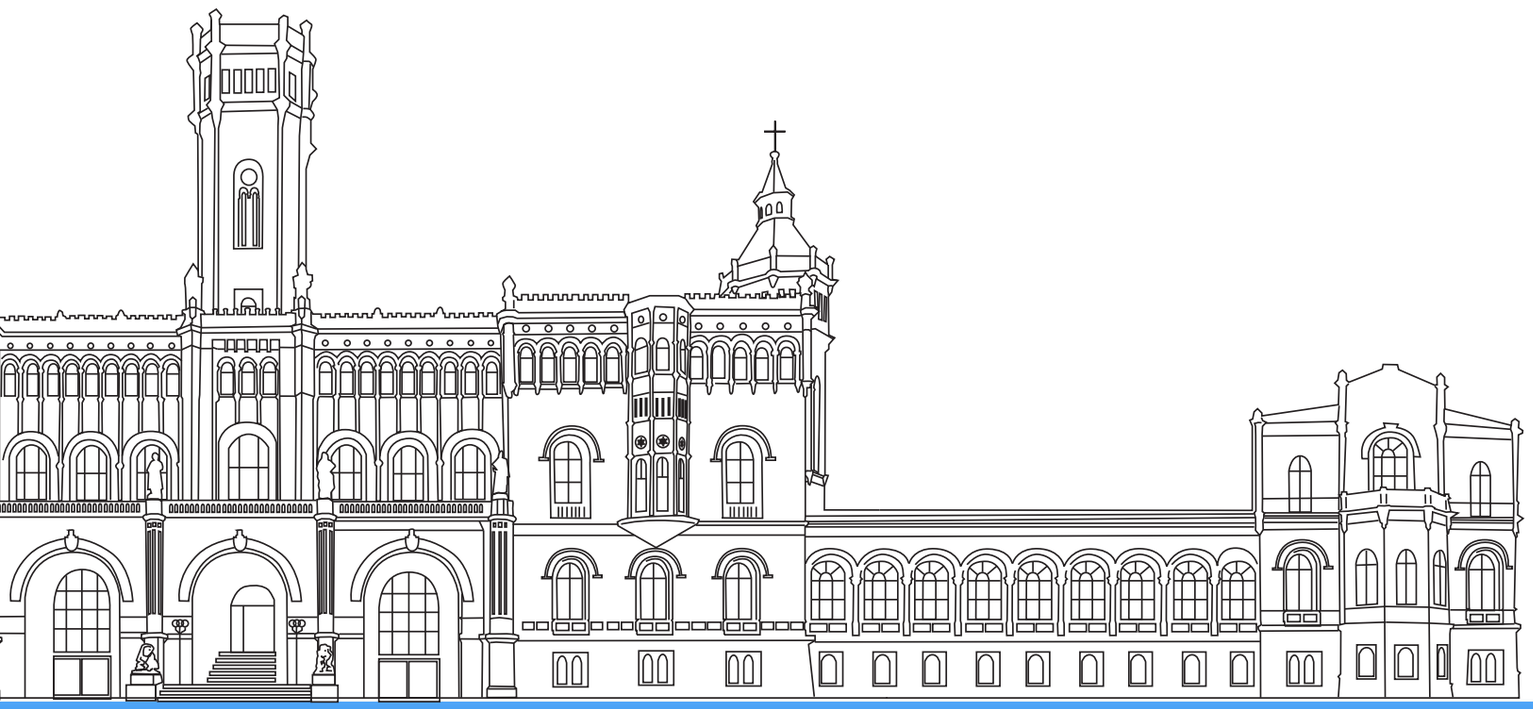

„Basic“ interferometers

Bloch Oscillations

Bragg scattering

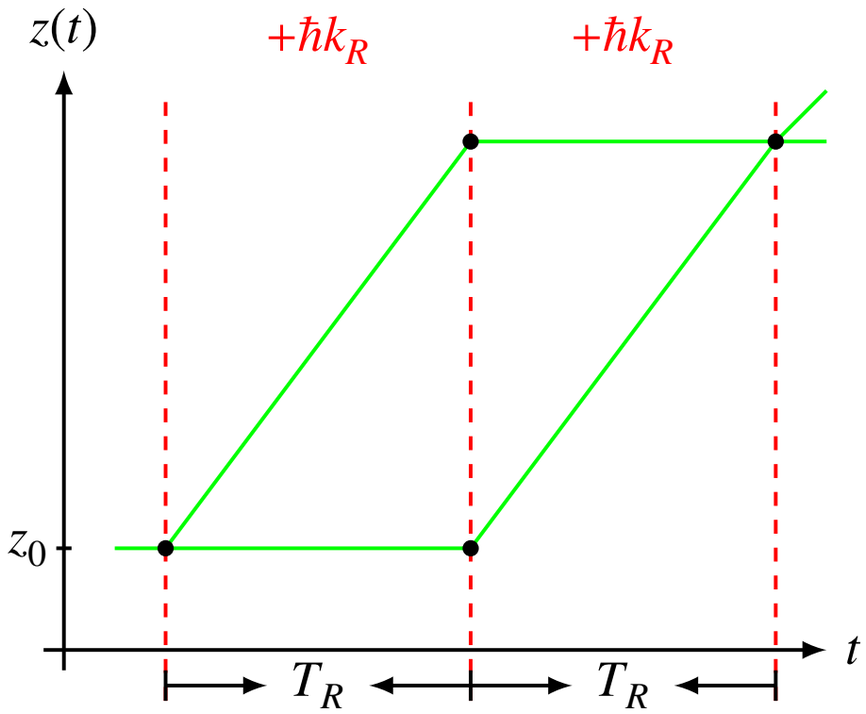

(a) Mach-Zehnder Interferometer (MZI)

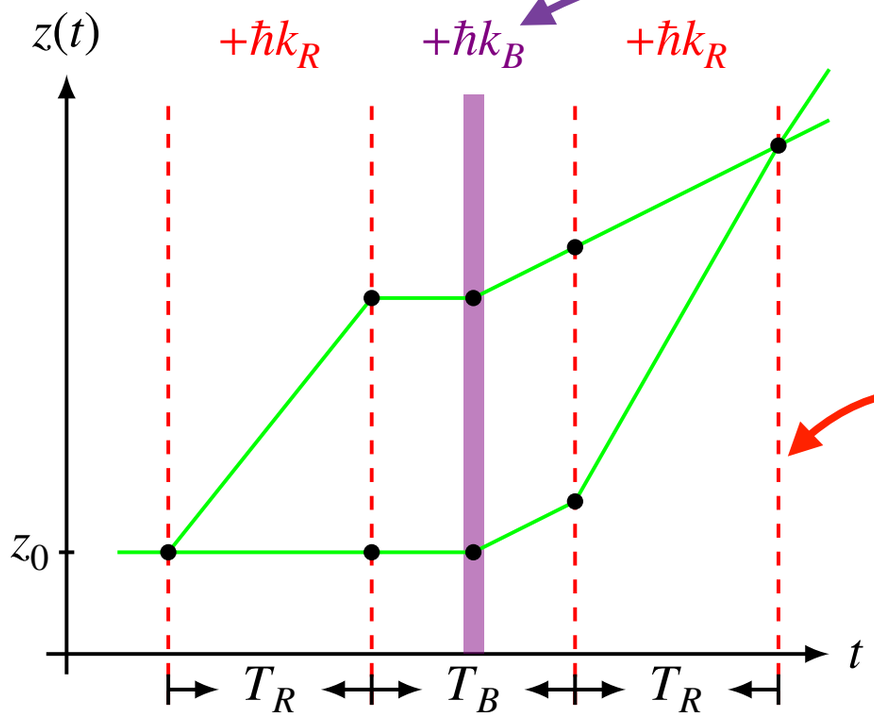

(b) Symmetric Ramsey-Bordé (SRBI)

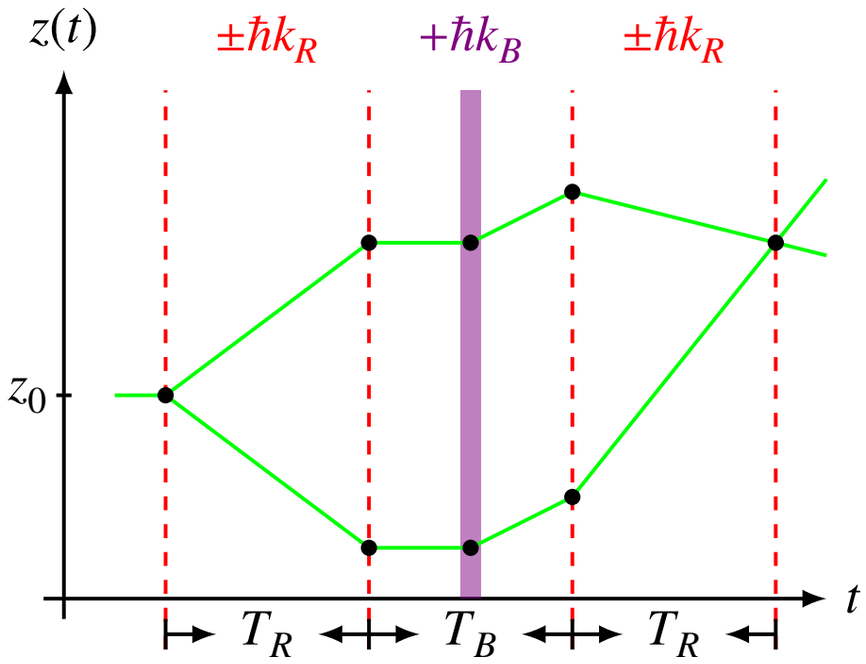

(c) Symmetric Double Diffraction (SDDI)

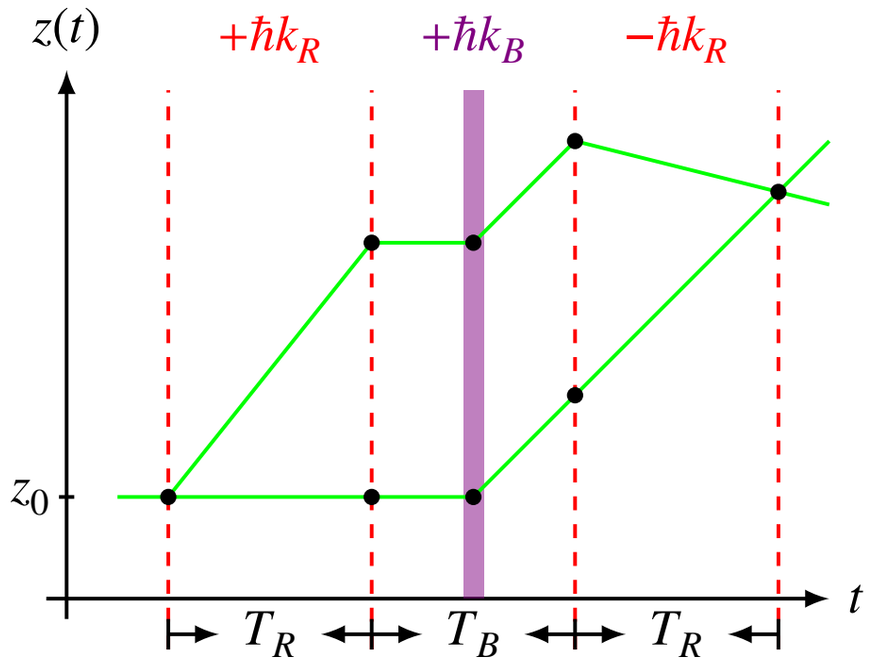

(d) Asymmetric Ramsey-Bordé (ARBI)

Dimensionless description

$$\Delta\Phi = g k_R T_R^2 = \frac{mc^2}{\hbar} T_R \cdot \frac{g T_R}{c} \cdot \frac{\hbar k_R}{mc}$$

$\sim 10^{-11}$

$\sim 10^{-8}$

Denote this as

$$\mathcal{O}(2) \approx 10^7 \,\mathrm{rad}$$

One can write **every** phase shift in an atom interferometer in this form!

Using this notation we can **systematically group** phase shifts!

Different example: $\Delta\Phi = g k_R \Gamma_0 T_R^4 = \omega_C T_R \cdot \frac{g T_R}{c} \cdot \frac{\hbar k_R}{mc} \cdot \Gamma_0 T_R^2$

Denote this as

$$\mathcal{O}(3) \approx 10^0 \,\mathrm{rad}$$

Dimensionless parameters (for now)

Parameter	Definition
$\mathcal{Z}_0$	$\frac{z_0}{cT_R}$
$\mathcal{V}_0$	$\frac{v_0}{c}$
$\mathcal{F}_\mathrm{R}$	$\frac{\hbar\omega_R}{mc^2}$
$\mathcal{G}_{1,i}$	$\frac{gT_i}{c}$
$\mathcal{G}_{2,i}$	$\Gamma_0 T_i^2$
$\mathcal{R}_i$	$\frac{\hbar k_i}{mc}$

Smaller than the others

Initial conditions: 10^{-8}

Recoil frequency: 10^{-20}

Gravitational potential: 10^{-8}

Recoil momentum: 10^{-11}–10^{-9}

Python algorithm

Created an open source Python algorithm that symbolically (!) calculates the phase shifts using **SymPy**.

```
# ~~~~~~~~~~~~~~~~~~~~~~~~~~~~~~~~~~~~~~~~~~~~~~~~~~~~~~~~~~~~~~~~~~~~~~~~~~~~
# ~~ Mach-Zehnder Interferometer (MZI) (3-pulse Interferometer) ~~
# ~~~~~~~~~~~~~~~~~~~~~~~~~~~~~~~~~~~~~~~~~~~~~~~~~~~~~~~~~~~~~~~~~~~~~~~~~~~~
```

Let me show it to you!

```
interfer
time_dec

bragg_quanta_upper_path = [0, 1, 0, 0]
bloch_quanta_upper_path = [0, 0, 0, 0]
bragg_quanta_lower_path = [0, 0, 1, 0]
bloch_quanta_lower_path = [0, 0, 0, 0]
```

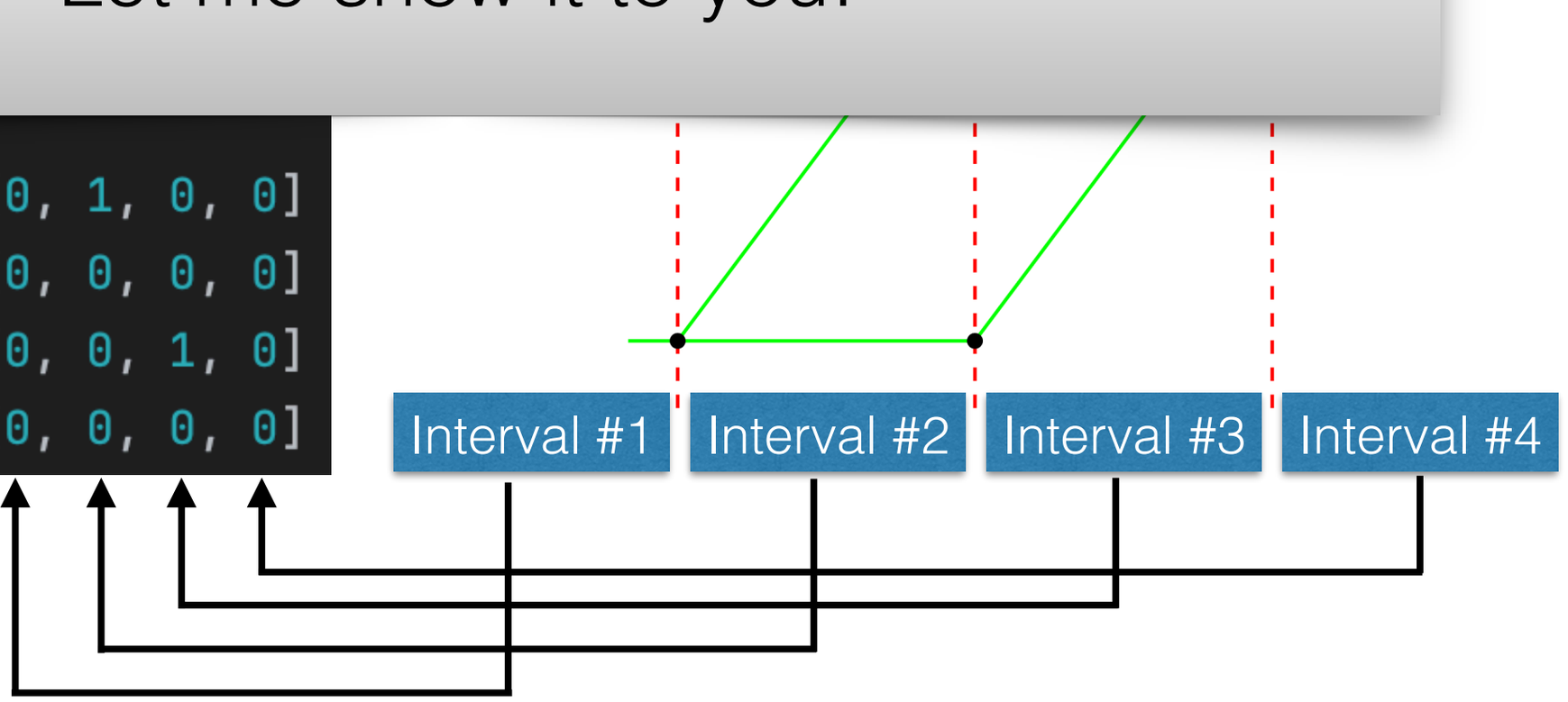

Python algorithm

	Included:	**Not included:**
Version #1	• GR effects • Doppler effect (1st and 2nd order) • Elastic scattering processes (Bragg, Bloch)	• Coriolis & Centrifugal effect • Finite speed of light (FSL) • Inelastic processes (Single photon, Raman) • 3D Analysis • Numerical Gravity Model
Version #2	• Added: Finite speed of light (FSL) • Added: Inelastic processes (Single photon, Raman) • Added: Numerical Gravity Model	• Coriolis & Centrifugal effect • 3D Analysis

Reference

If you want to read more about this

Python algorithm

Atom interferometers in weakly curved spacetimes using Bragg diffraction and Bloch oscillations

Python algorithm of: Atom interferometers in weakly curved spacetimes using Bragg diffraction and Bloch oscillations

This dataset contains the Python algorithm to reproduce all results in this manuscript:

Instructions on how to run the code can be found in the ReadMe.md file.

GitLab Clone Link to the repository: https://gitlab.uni-hannover.de/michael.werner/atom-interferometers-in-weakly-curved-spacetimes-using-bragg-diffraction-and-bloch-oscillations.git

Data and Resources

PPN_Python_Atom_IF_Analysis.zip
Complete dataset: Zip file of the Python algorithm including results for... File size: 3.5 MByte — Explore

README.md
ReadMe file. File size: 7.7 KByte — Explore

atom interferometry | physics

PHYSICAL REVIEW D **109,** 022008 (2024)

Atom interferometers in weakly curved spacetimes using Bragg diffraction and Bloch oscillations

Michael Werner,[1] Philip K. Schwartz,[1] Jan-Niclas Kirsten-Siemß,[1,2] Naceur Gaaloul,[2] Domenico Giulini,[1,3] and Klemens Hammerer[1]
[1]*Institut für Theoretische Physik, Leibniz Universität Hannover, Appelstraße 2, 30167 Hannover, Germany*
[2]*Institut für Quantenoptik, Leibniz Universität Hannover, Welfengarten 1, 30167 Hannover, Germany*
[3]*Zentrum für Angewandte Raumfahrttechnologie und Mikrogravitation, Universität Bremen, Am Fallturm 1, 28359 Bremen, Germany*

(Received 18 October 2023; accepted 21 November 2023; published 29 January 2024)

We present a systematic approach to determine all relativistic phases up to $\mathcal{O}(c^{-2})$ in light-pulse atom interferometers in weakly curved spacetime that are based on elastic scattering—namely, Bragg diffraction and Bloch oscillations. Our analysis is derived from first principles using the parametrized post-Newtonian formalism. In the treatment developed here, we derive algebraic expressions for relativistic phases for arbitrary interferometer geometries in an automated manner. As case studies, we consider symmetric and antisymmetric Ramsey-Bordé interferometers, as well as a symmetric double diffraction interferometer with baseline lengths of 10 m and 100 m. We compare our results to previous calculations conducted for a Mach-Zehnder interferometer.

DOI: 10.1103/PhysRevD.109.022008

I. INTRODUCTION

Atom interferometers (IFs), at the forefront of quantum metrology, are highly precise instruments widely utilized in various research domains. They have been employed in diverse fields, including the determination of the fine-structure constant [1,2], serving as quantum sensors for measuring the gravitational field of the Earth [3–6], proposed measurements of gravitational waves [7–10], and investigations of fundamental physics and alternative gravitational models [11–15], as well as measurements of time dilation and gravitational redshift [16–20].

The interpretation of measurements of the gravitational redshift has ignited extensive discussions regarding the influence of relativistic effects in atom IFs [21–24]. These discussions have underscored the need for interferometry with internal superposition states [19,20] enabling the effective detection of gravitational redshift effects. As a result, there has been significant research focus on IFs employing inelastic scattering processes, such as single-photon or Raman transitions, commonly referred to as "clock interferometry." However, inelastic scattering introduces additional systematic effects due to the different internal atomic states. In contrast, atom IFs based on elastic scattering processes, such as Bragg diffraction [25,26] and Bloch oscillations [27,28], currently exhibit the highest sensitivity. This advancement has facilitated groundbreaking measurements, such as the precise determination of atomic recoil—and, consequently, the fine-structure constant—with unprecedented accuracy [2]. The gravitational redshift cannot be directly measured with these IFs; it is worth noting that phases involving relativistic effects and even extensions to the standard model (SME) can still manifest in these atom IFs [29,30].

Dimopoulos *et al.* [31,32] presented the determination and detailed listing of phases induced by special and general relativistic effects specifically for the Mach-Zehnder IF. However, the laborious algebraic calculations involved make it difficult to reproduce and extend these results to more general IF geometries. Here, we propose a systematic framework for computing relativistic phases in arbitrary atom IFs realized by elastic scattering. Our approach employs rigorous expansions in relevant small parameters, implemented through computer algebra in Python [33]. This enables automated algebraic calculations of relativistic phases up to the desired order of accuracy. We compute and display the phases for three common IF geometries: the symmetric Ramsey-Bordé interferometer (SRBI), antisymmetric Ramsey-Bordé interferometer (ARBI), and symmetric double diffraction interferometer (SDDI). The computer algorithm is, however, capable of calculating phases for more general IF geometries. For each geometry, we algebraically list and quantitatively illustrate the leading relativistic phases. Our analysis focuses on atom IFs with baseline lengths of 10 m and 100 m, inspired by numerous operational or under-development setups [10,34–38]. Furthermore, we provide a detailed comparison

For the rest of today we'll concentrate on spiciness level two:

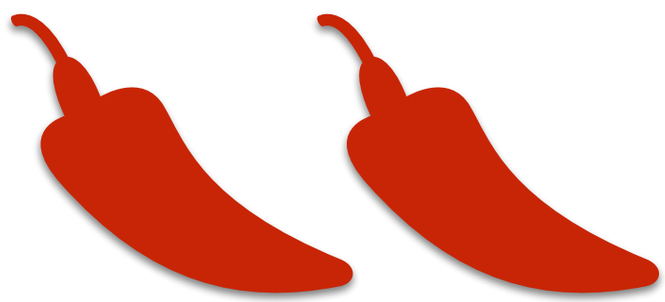

3. Measurements of gravitational curvature

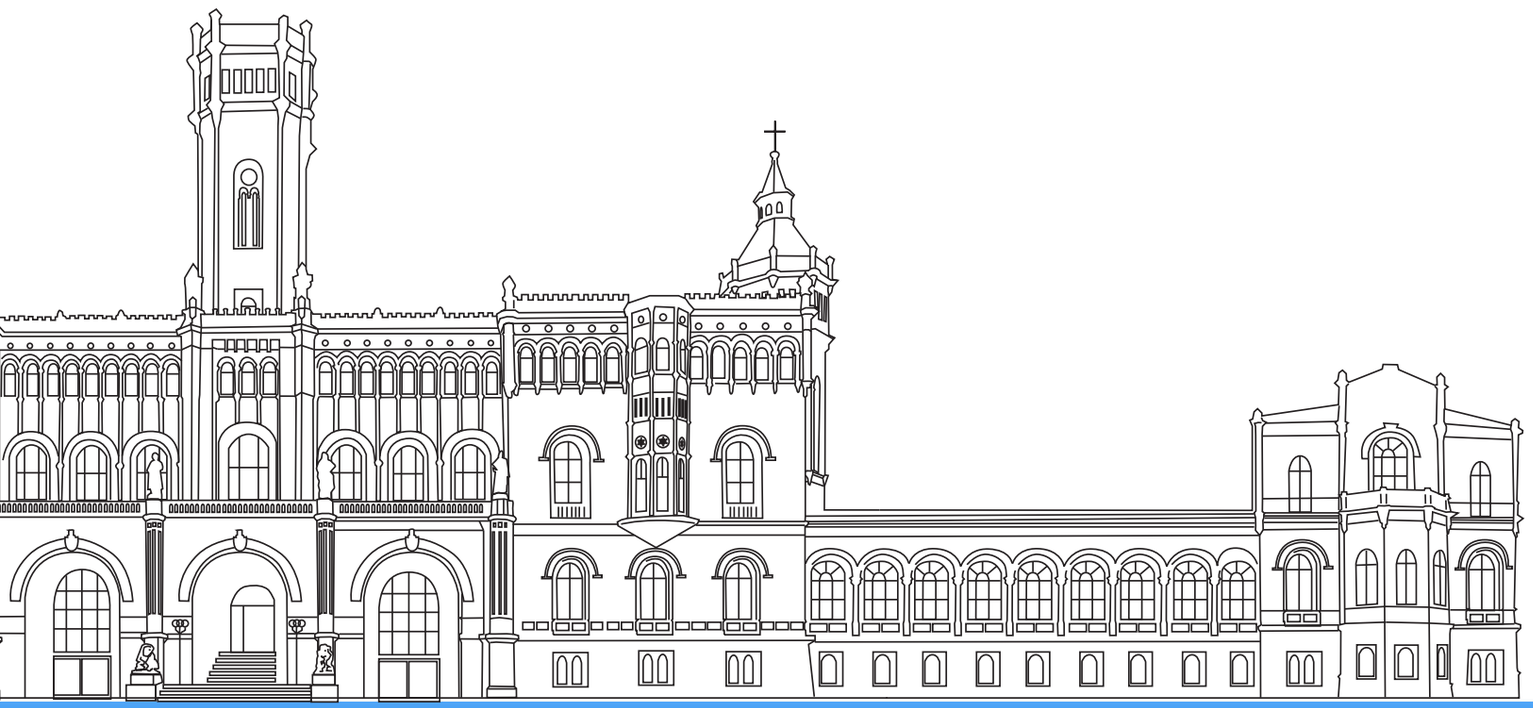

Phase shift results (without FSL)

Phases in units of ω_C							
#	Order	Proportionality	SRBI	SDDI	ARBI	α	Origin
1	$O(2)$	$\mathcal{G}_{1,\mathrm{R}}\mathcal{R}_{\mathrm{R}}$	$T_B + T_R$	$2T_B + 2T_R$	$T_B + T_R$	2	Non-relativistic
2		$\mathcal{R}_{\mathrm{R}}^2$	0	0	T_R	1	
3		$\mathcal{R}_{\mathrm{R}}\mathcal{R}_{\mathrm{B}}$	$-T_R$	$-2T_R$	$-T_R$	1	
4	$O(3)$	$\mathcal{R}_{\mathrm{R}}\mathcal{Z}_0\mathcal{G}_{2,\mathrm{R}}$	$-T_B - T_R$	$-2T_B - 2T_R$	$-T_B - T_R$	2	Gravity gradient
5		$\mathcal{R}_{\mathrm{R}}\mathcal{V}_0\mathcal{G}_{2,\mathrm{R}}$	$-\frac{3}{2}T_B - T_R$	$-3T_B - 2T_R$	$-\frac{3}{2}T_B - T_R$	3	
6		$\mathcal{R}_{\mathrm{R}}\mathcal{R}_{\mathrm{B}}\mathcal{G}_{2,\mathrm{R}}$	$-\frac{1}{4}T_B - \frac{1}{6}T_R$	$-\frac{1}{2}T_B - \frac{1}{3}T_R$	$-\frac{1}{4}T_B - \frac{1}{6}T_R$	4	
7		$\mathcal{R}_{\mathrm{R}}\mathcal{G}_{1,\mathrm{R}}\mathcal{G}_{2,\mathrm{R}}$	$\frac{7}{6}T_B + \frac{7}{12}T_R$	$\frac{7}{3}T_B + \frac{7}{6}T_R$	$\frac{7}{6}T_B + \frac{7}{12}T_R$	4	
8		$\mathcal{R}_{\mathrm{R}}^2\mathcal{G}_{2,\mathrm{R}}$	$-\frac{1}{2}T_B - \frac{1}{2}T_R$	0	$-\frac{1}{2}T_B - \frac{1}{3}T_R$	3	
9		$\mathcal{R}_{\mathrm{R}}\mathcal{V}_0\mathcal{G}_{2,\mathrm{B}}$	$-\frac{1}{2}T_R$	$-T_R$	$-\frac{1}{2}T_R$	3	
10		$\mathcal{R}_{\mathrm{R}}\mathcal{R}_{\mathrm{B}}\mathcal{G}_{2,\mathrm{B}}$	$-\frac{1}{8}T_R$	$-\frac{1}{4}T_R$	$-\frac{1}{8}T_R$	3	
11		$\mathcal{R}_{\mathrm{R}}\mathcal{G}_{1,\mathrm{R}}\mathcal{G}_{2,\mathrm{B}}$	$\frac{1}{6}T_B + \frac{3}{4}T_R$	$\frac{1}{3}T_B + \frac{3}{2}T_R$	$\frac{1}{6}T_B + \frac{3}{4}T_R$	4	
12		$\mathcal{F}_{\mathrm{R}}\mathcal{G}_{1,\mathrm{R}}^2$	$-\frac{9}{2}T_B - 3T_R$	$-9T_B - 6T_R$	$-\frac{9}{2}T_B - 3T_R$	3	Doppler effect
13		$\mathcal{F}_{\mathrm{R}}\mathcal{G}_{1,\mathrm{R}}\mathcal{V}_0$	$3T_B + 3T_R$	$6T_B + 6T_R$	$3T_B + 3T_R$	2	
14		$\mathcal{F}_{\mathrm{R}}\mathcal{G}_{1,\mathrm{R}}\mathcal{G}_{1,\mathrm{B}}$	$-\frac{3}{2}T_B$	$-3T_B$	$-\frac{3}{2}T_B$	3	
15		$\mathcal{F}_{\mathrm{R}}\mathcal{R}_{\mathrm{B}}\mathcal{G}_{1,\mathrm{R}}$	$\frac{5}{2}T_B + \frac{7}{2}T_R$	$5T_B + 7T_R$	$\frac{5}{2}T_B + \frac{7}{2}T_R$	2	
16		$\mathcal{F}_{\mathrm{R}}\mathcal{R}_{\mathrm{B}}^2$	$-T_R$	$-2T_R$	$-T_R$	1	
17		$\mathcal{F}_{\mathrm{R}}\mathcal{R}_{\mathrm{B}}\mathcal{V}_0$	$-2T_R$	$-4T_R$	$-2T_R$	1	
18		$\mathcal{F}_{\mathrm{R}}\mathcal{R}_{\mathrm{R}}^2$	0	$2T_R$	T_R	1	
19		$\mathcal{F}_{\mathrm{R}}\mathcal{R}_{\mathrm{R}}\mathcal{G}_{1,\mathrm{B}}$	$\frac{1}{2}T_B$	0	$-\frac{1}{2}T_B$	2	
20		$\mathcal{F}_{\mathrm{R}}\mathcal{R}_{\mathrm{R}}\mathcal{G}_{1,\mathrm{R}}$	$3T_B - \frac{5}{2}T_R$	0	$-3T_B + \frac{9}{2}T_R$	2	
21		$\mathcal{F}_{\mathrm{R}}\mathcal{R}_{\mathrm{R}}\mathcal{R}_{\mathrm{B}}$	$-\frac{1}{2}T_B + 2T_R$	0	$\frac{1}{2}T_B - 2T_R$	1	
22		$\mathcal{F}_{\mathrm{R}}\mathcal{R}_{\mathrm{R}}\mathcal{V}_0$	$-T_B - T_R$	0	$T_B + 5T_R$	1	
23		$\mathcal{F}_{\mathrm{R}}\mathcal{R}_{\mathrm{R}}\mathcal{Z}_0$	0	0	$2T_R$	1	

$$(2T_B + 2T_R) \cdot \omega_C \cdot \underbrace{\mathcal{G}_{1,\mathrm{R}}\mathcal{R}_{\mathrm{R}}}_{\mathcal{O}(2)} = 2gk_R \underbrace{T_R(T_B + T_R)}_{\alpha = 2}$$

Small

Phase shift results (without FSL)

Proportionality	SRBI	SDDI	ARBI	α
$\mathcal{G}_{1,\mathrm{R}}\mathcal{R}_{\mathrm{R}}$	$T_B + T_R$	$2T_B + 2T_R$	$T_B + T_R$	2
$\mathcal{R}_{\mathrm{R}}^2$	0	0	T_R	1
$\mathcal{R}_{\mathrm{R}}\mathcal{R}_{\mathrm{B}}$	$-T_R$	$-2T_R$	$-T_R$	1
$\mathcal{R}_{\mathrm{R}}\mathcal{Z}_0\mathcal{G}_{2,\mathrm{R}}$	$-T_B - T_R$	$-2T_B - 2T_R$	$-T_B - T_R$	2
$\mathcal{R}_{\mathrm{R}}\mathcal{V}_0\mathcal{G}_{2,\mathrm{R}}$	$-\frac{3}{2}T_B - T_R$	$-3T_B - 2T_R$	$-\frac{3}{2}T_B - T_R$	3
$\mathcal{R}_{\mathrm{R}}\mathcal{R}_{\mathrm{B}}\mathcal{G}_{2,\mathrm{R}}$	$-\frac{1}{4}T_B - \frac{1}{6}T_R$	$-\frac{1}{2}T_B - \frac{1}{3}T_R$	$-\frac{1}{4}T_B - \frac{1}{6}T_R$	4
$\mathcal{R}_{\mathrm{R}}\mathcal{G}_{1,\mathrm{R}}\mathcal{G}_{2,\mathrm{R}}$	$\frac{7}{6}T_B + \frac{7}{12}T_R$	$\frac{7}{3}T_B + \frac{7}{6}T_R$	$\frac{7}{6}T_B + \frac{7}{12}T_R$	4
$\mathcal{R}_{\mathrm{R}}^2\mathcal{G}_{2,\mathrm{R}}$	$-\frac{1}{2}T_B - \frac{1}{2}T_R$	0	$-\frac{1}{2}T_B - \frac{1}{3}T_R$	3
$\mathcal{R}_{\mathrm{R}}\mathcal{V}_0\mathcal{G}_{2,\mathrm{B}}$	$-\frac{1}{2}T_R$	$-T_R$	$-\frac{1}{2}T_R$	3
$\mathcal{R}_{\mathrm{R}}\mathcal{R}_{\mathrm{B}}\mathcal{G}_{2,\mathrm{B}}$	$-\frac{1}{8}T_R$	$-\frac{1}{4}T_R$	$-\frac{1}{8}T_R$	3
$\mathcal{R}_{\mathrm{R}}\mathcal{G}_{1,\mathrm{R}}\mathcal{G}_{2,\mathrm{B}}$	$\frac{1}{6}T_B + \frac{3}{4}T_R$	$\frac{1}{3}T_B + \frac{3}{2}T_R$	$\frac{1}{6}T_B + \frac{3}{4}T_R$	4

Interesting asymmetry

$$\omega_C T_R \cdot \mathcal{R}_{\mathrm{R}}^2 \mathcal{G}_{2,\mathrm{R}} = \frac{\hbar k_R^2 \Gamma_0 T_R^3}{m}$$

Most phases scale with a factor of two (spacetime area). But this one not!

Can we use this to gain information about the gravity gradient?

Co-located Gradiometric Interferometer (CGI)

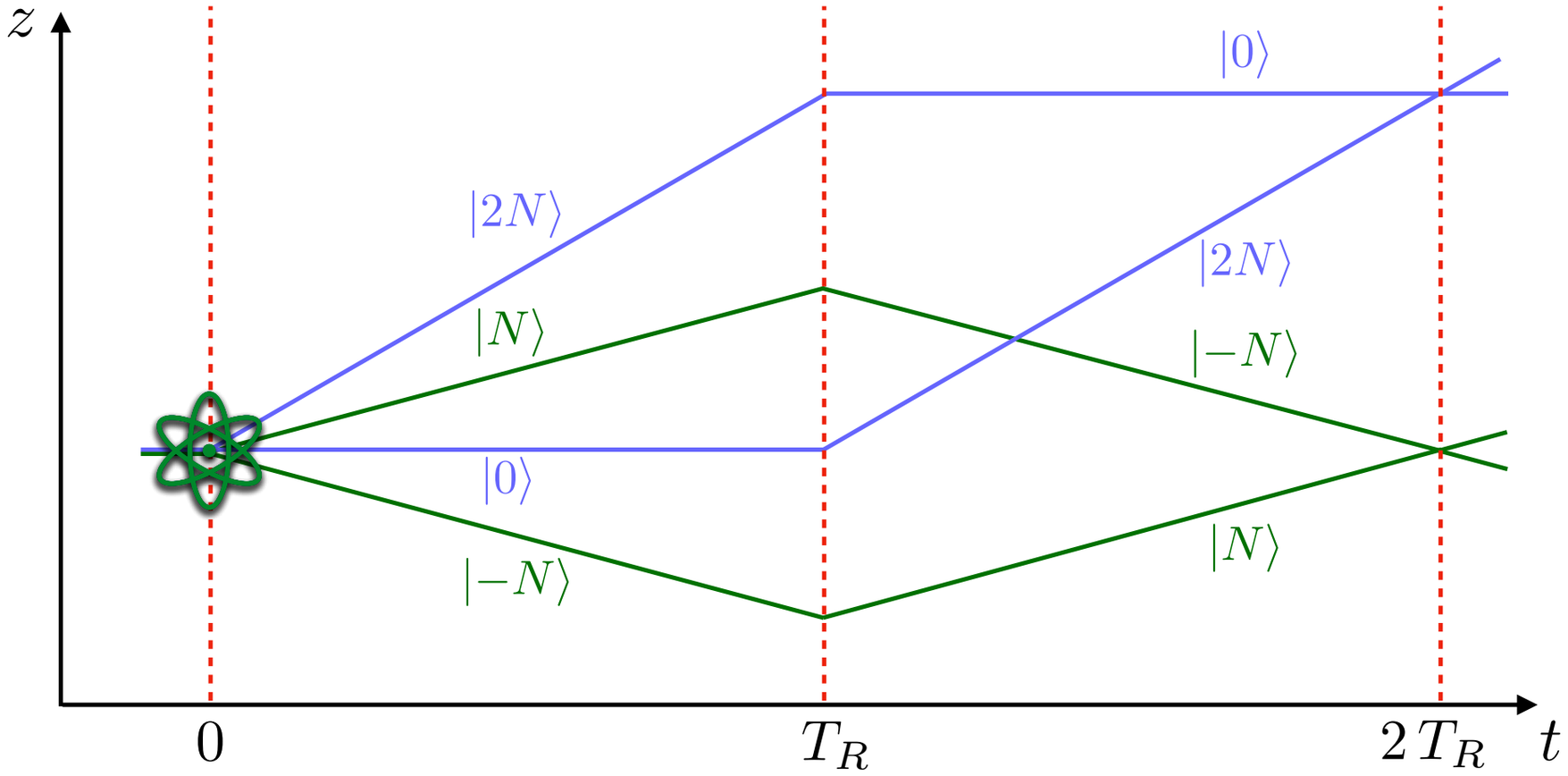

MZI

SDDI

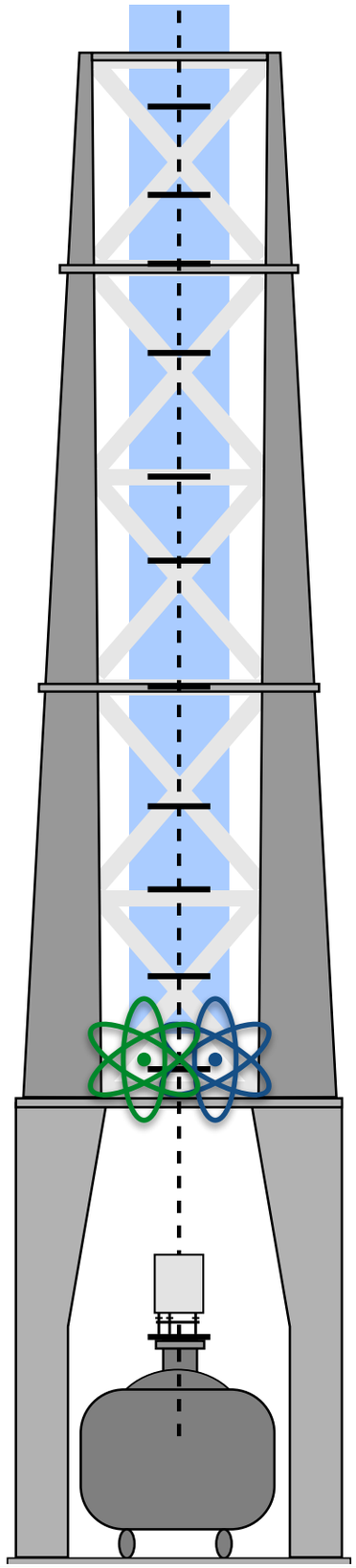

VLBAI figure adapted from Schilling et al. „Gravity field modelling for the Hannover 10 m atom interferometer“

CGI phase comparison

Differential phase shift is proportional to the gravity gradient

$$\Delta\Phi = -2N^2\mathcal{G}_{2,\mathrm{R}}\mathcal{R}_{\mathrm{R}}^2 = -2\frac{N^2\hbar k_R^2\Gamma_0 T_R^3}{m} = f\cdot\Gamma_0$$

Phase comparison of a MZI and a SDDI in a CGI configuration (no FSL phases)

MZI	SDDI	Phase	Phase	Magnitude [rad]	Differential signal
2	2	$Nk_R g T_R^2$	$N\mathcal{R}_{\mathrm{R}}\mathcal{G}_{1,\mathrm{R}}$	1.4×10^{7}	0
−2	−2	$Nk_R z_0\Gamma_0 T_R^2$	$N\mathcal{Z}_0\mathcal{G}_{2,\mathrm{R}}\mathcal{R}_{\mathrm{R}}$	20	0
−2	−2	$Nk_R v_0\Gamma_0 T_R^3$	$N\mathcal{V}_0\mathcal{G}_{2,\mathrm{R}}\mathcal{R}_{\mathrm{R}}$	14	0
$\frac{7}{6}$	$\frac{7}{6}$	$Nk_R g\Gamma_0 T_R^4$	$N\mathcal{G}_{1,\mathrm{R}}\mathcal{G}_{2,\mathrm{R}}\mathcal{R}_{\mathrm{R}}$	14	0
−2	0	$\frac{N^2\hbar k_R^2\Gamma_0 T_R^3}{m}$	$N^2\mathcal{G}_{2,\mathrm{R}}\mathcal{R}_{\mathrm{R}}^2$	1.5×10^{-2}	−2
−12	−12	$\frac{N\omega_R g^2 T_R^3}{c^2}$	$N\mathcal{G}_{1,\mathrm{R}}^2\mathcal{F}_{\mathrm{R}}$	2.3×10^{-9}	0
12	12	$\frac{N\omega_R g v_0 T_R^2}{c^2}$	$N\mathcal{F}_{\mathrm{R}}\mathcal{G}_{1,\mathrm{R}}\mathcal{V}_0$	2.4×10^{-9}	0

$$f = -2\frac{N^2\hbar k_R^2 T_R^3}{m}$$

Phase shift is small (a few mrad).

What about FSL?
Does this give us a problem?

Finite speed of light (FSL)

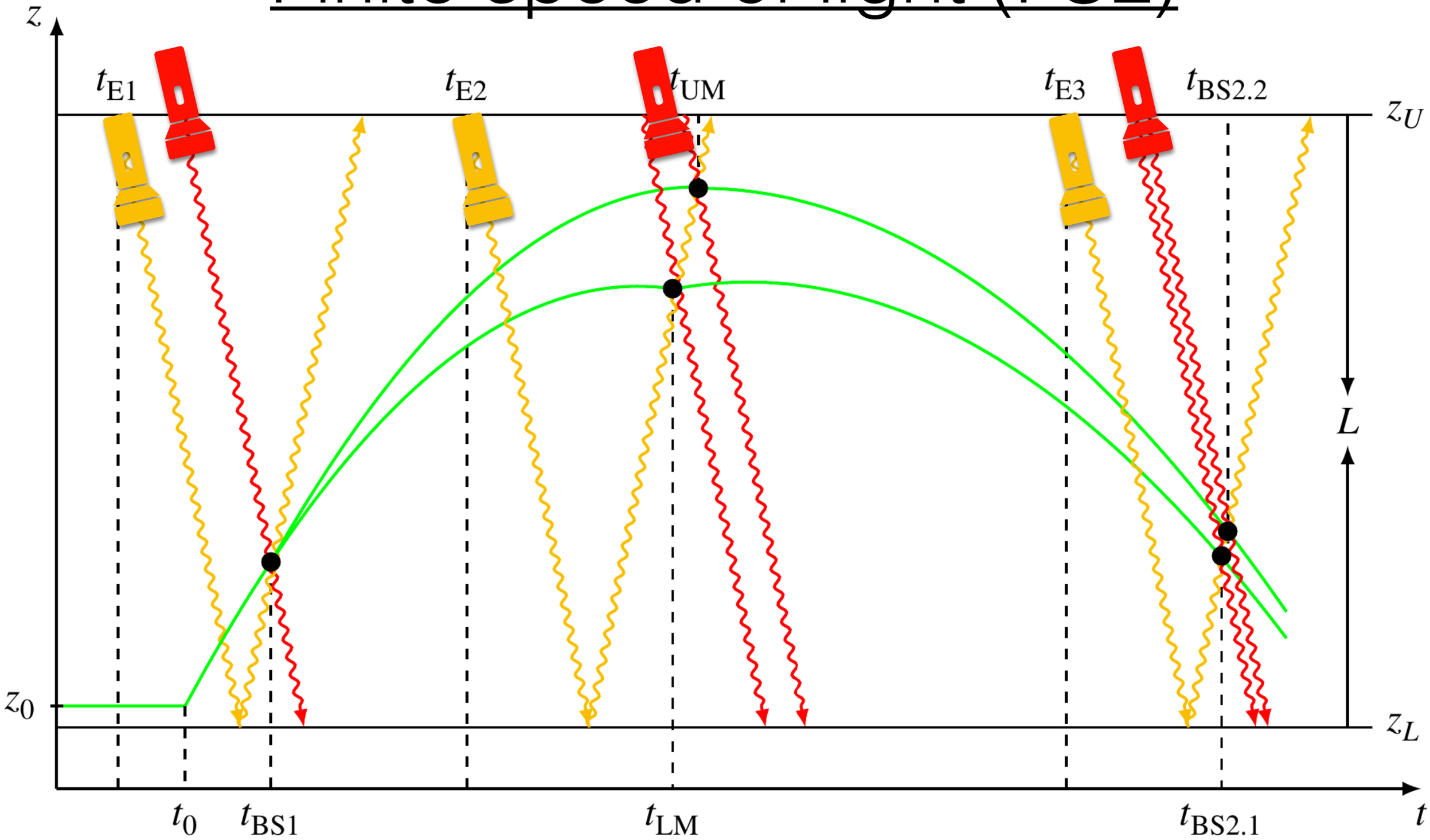

Example: Two photon Bragg transitions

Finite speed of light mitigation

Example: Two photon Bragg transitions

Can we mitigate this?

$$\Delta\Phi_{\mathrm{FSL}} = \frac{4\hbar N^2 k^2 T_R}{mc}\left(4gT_R - v_0 - \frac{N\hbar k}{m}\right) + \Delta\Phi_0,$$

with a constant shift $\Delta\Phi_0 = \frac{2\hbar N^2 k^2}{mc}(2z_{\mathrm{L}} - z_0 - z_{\mathrm{U}}).$

„Lower laser“ (Or: Mirror position,…)

„Upper laser“

Finite speed of light mitigation

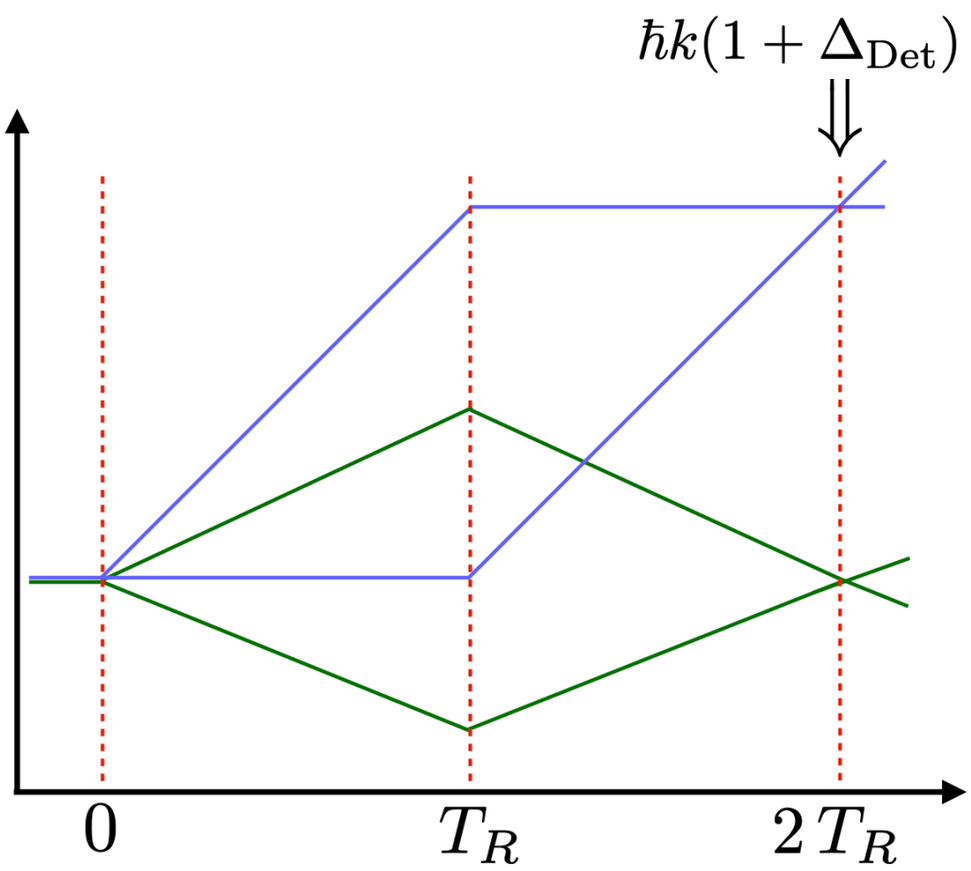

Alter the last AIF pulse by:

$$\Delta_{\mathrm{Det}}(v_0, T_R) = 2\frac{v_0 + \frac{\hbar k}{m} - 4gT_R}{v_0 + \frac{\hbar k}{m} - gT_R}\frac{\hbar k}{mc}$$

This frequency chirp (~100 MHz) nullifies the FSL phase!

Looks interesting so far, but the gravitational field is very idealised…

Complex gravitational fields

Consider $\phi(z) = \phi_0 + gz + \sum_{n=2} \frac{\phi^{(n)}}{n!} z^n$

$\phi^{(2)} = -\Gamma_0$
$\phi^{(3)} = \Lambda_0$

with a non-trivial $\Gamma(z) = \partial_z^2 \phi(z)$ = Gravitational curvature

- Example: VLBAI Hannover

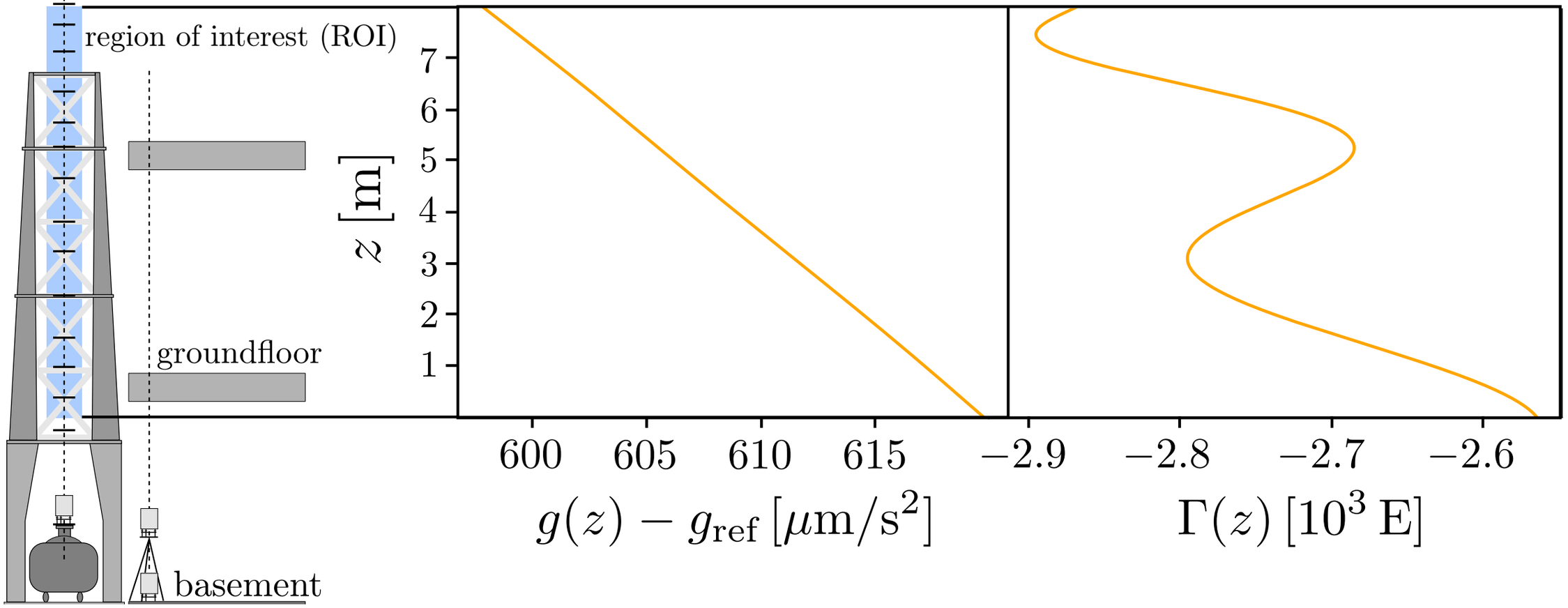

CGI: Numerical simulation in VLBAI

CGI Phase

Gravitational Curvature

Intuitively clear: the atoms „average“ gravity along their trajectory.

But how exactly?

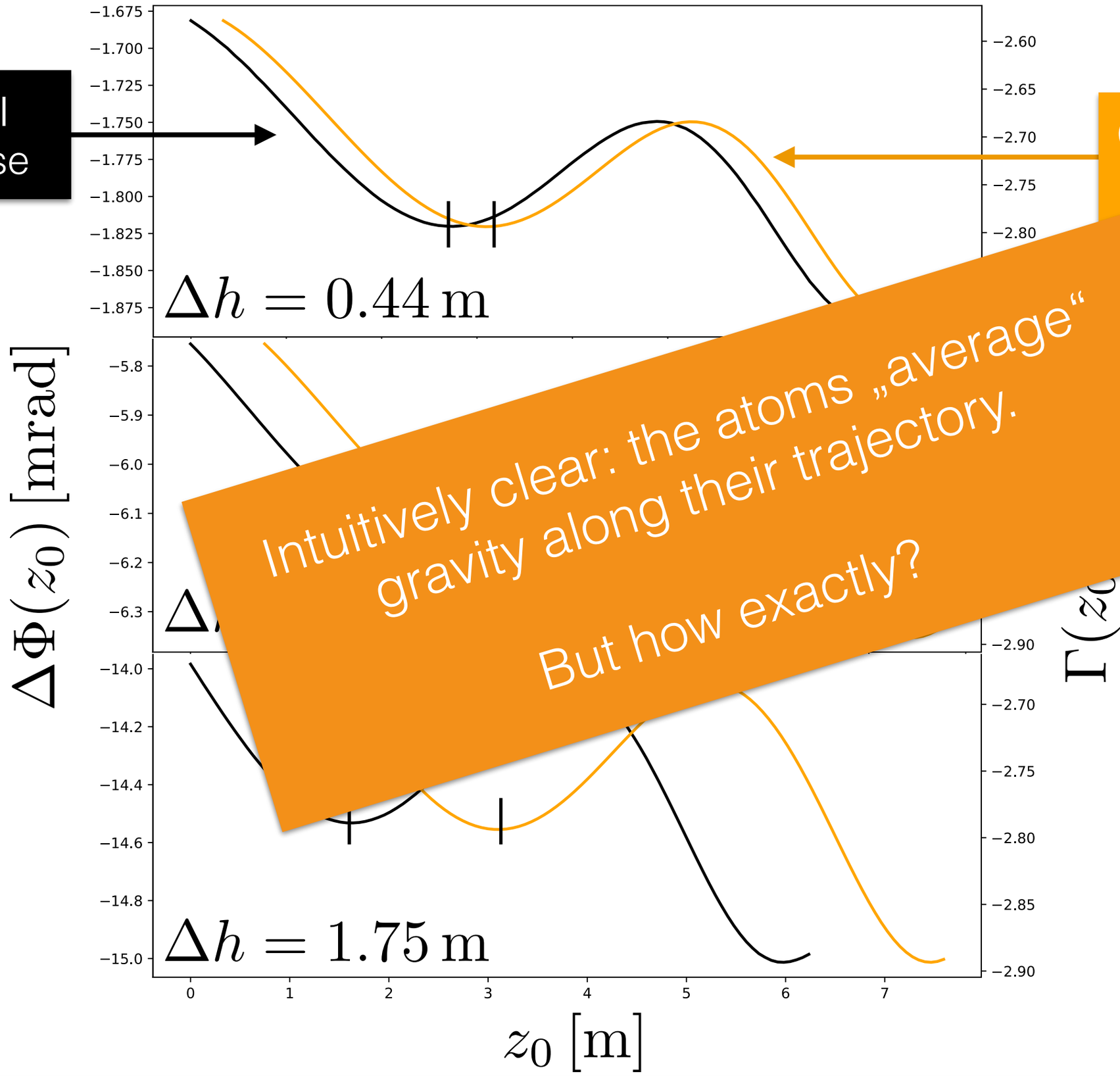

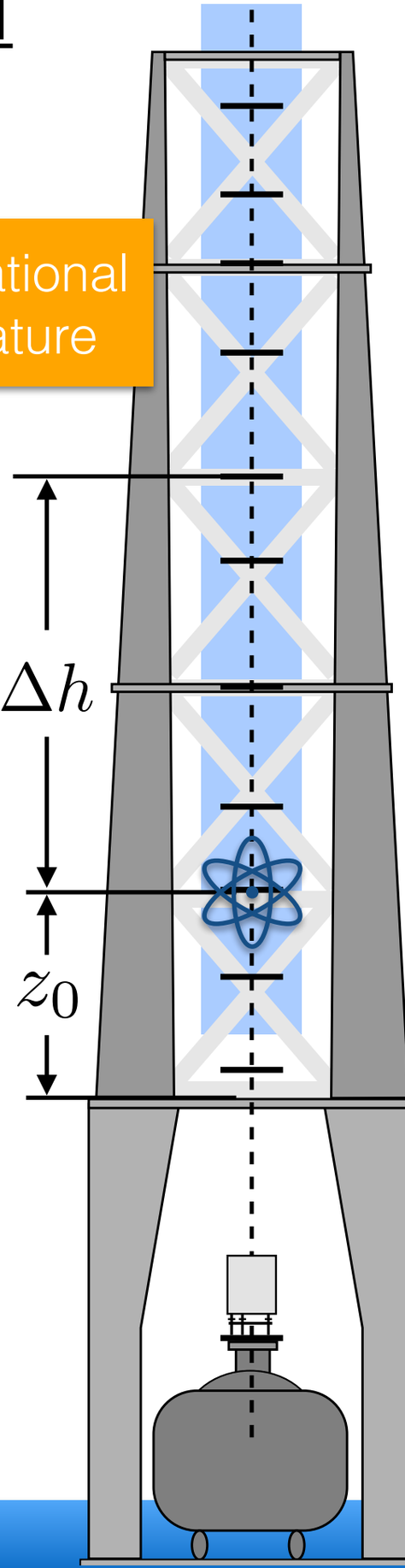

Averaging gravity

Where are the atoms „on average“?

Answer: It depends on the averaging process!

$$\|z(t)\|_n = \left(\frac{1}{2T_R} \int_0^{2T_R} |z(t) - z_0|^n \right)^{1/n}$$

n	1	2	3	4	5
$\|z(t)\|_n$	0.66 Δh	0.73 Δh	0.77 Δh	0.79 Δh	0.82 Δh

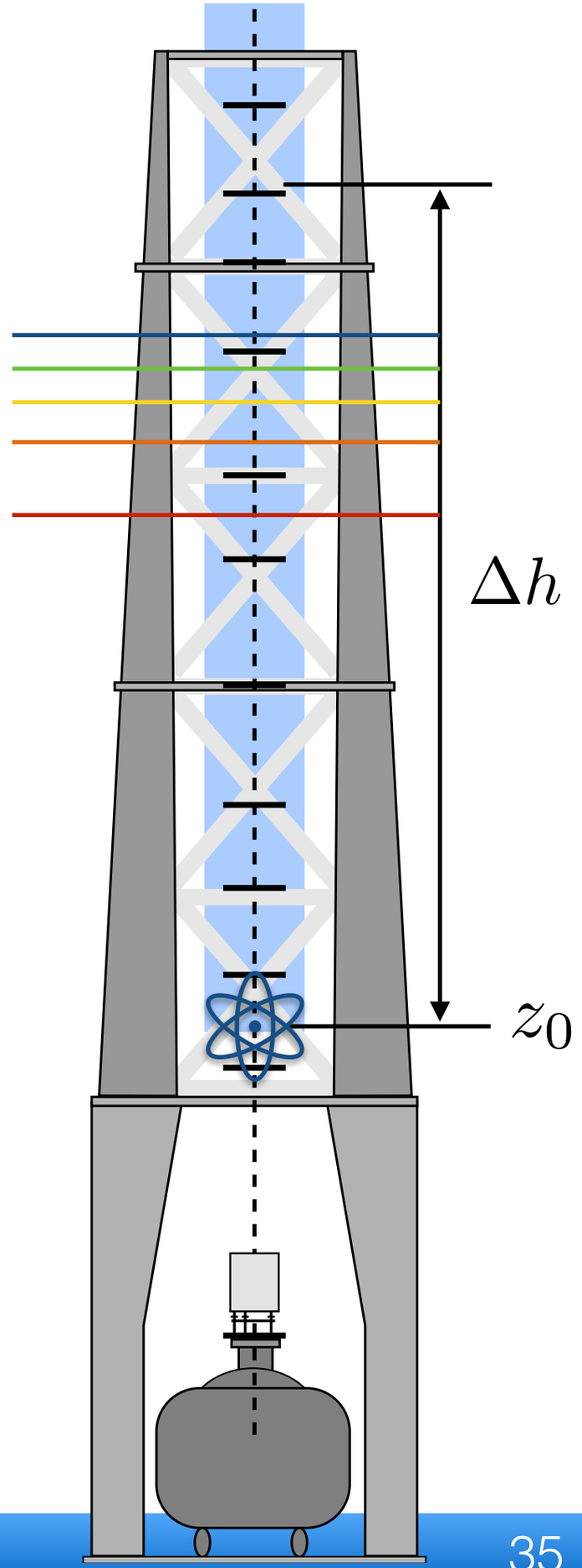

Estimator for grav. curvature

We can now define a novel estimator $\hat{\Gamma}(z_0)$ for the grav. curvature:

Step 1: Convert phase to grav. curvature using the scale factor.

$$\hat{\Gamma}(z_0) = \frac{\Delta\Phi(z_0)}{f}$$

Step 2: Shift the height via the **cubic** mean of the trajectory.

$$\hat{\Gamma}(z_0) = \frac{\Delta\Phi(z_0 - \|z(t)\|_3)}{f}$$

Reminder:

$$f = -2\frac{N^2\hbar k_R^2 T_R^3}{m}$$

Motivation for the **cubic** mean.

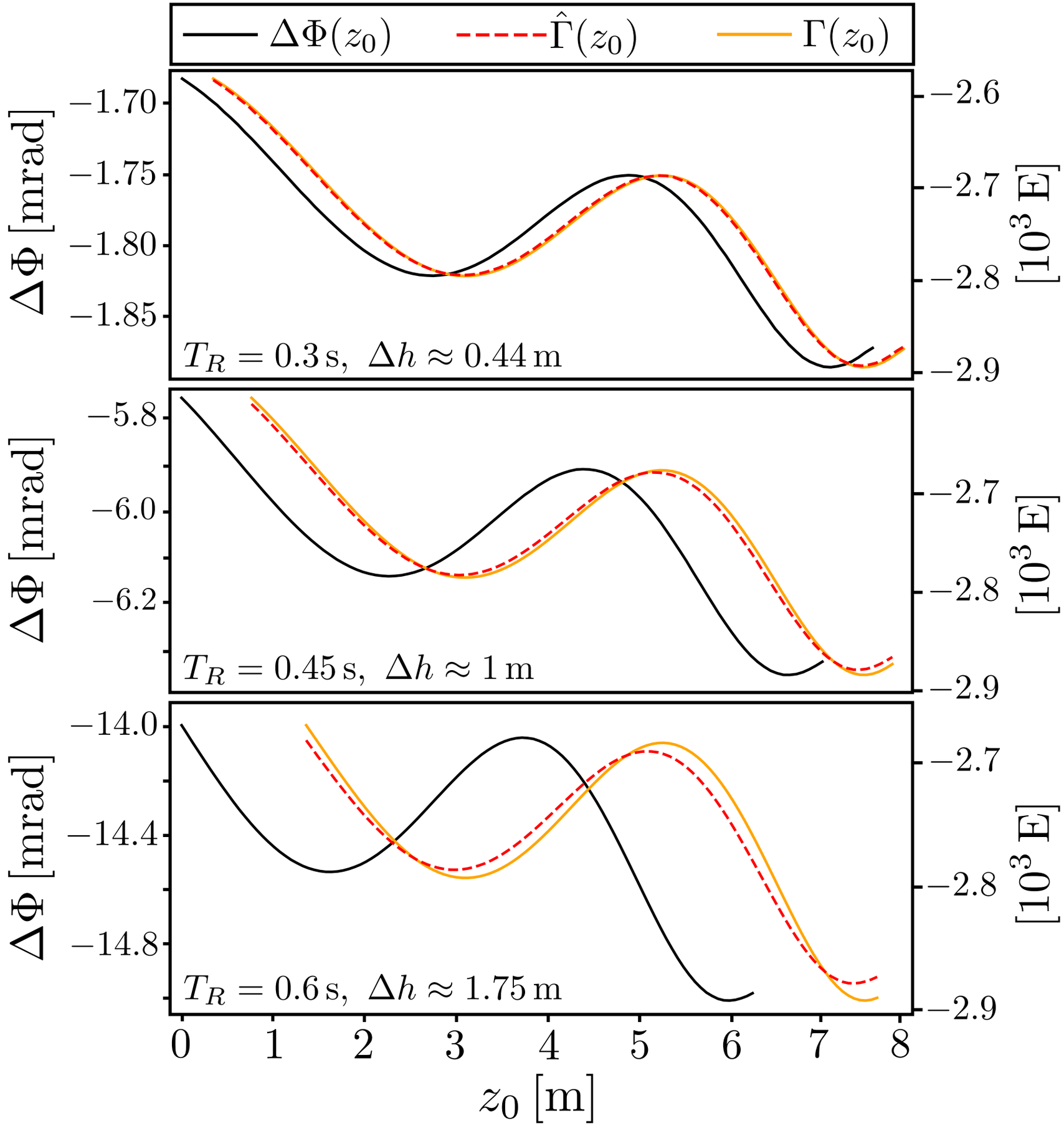
$\Delta\Phi(z_0)$
$\hat{\Gamma}(z_0)$
$\Gamma(z_0)$
$\Delta\Phi$ [mrad]
$[10^3\,\mathrm{E}]$
$T_R = 0.3\,\mathrm{s},\ \Delta h \approx 0.44\,\mathrm{m}$
$T_R = 0.45\,\mathrm{s},\ \Delta h \approx 1\,\mathrm{m}$
$T_R = 0.6\,\mathrm{s},\ \Delta h \approx 1.75\,\mathrm{m}$
z_0 [m]

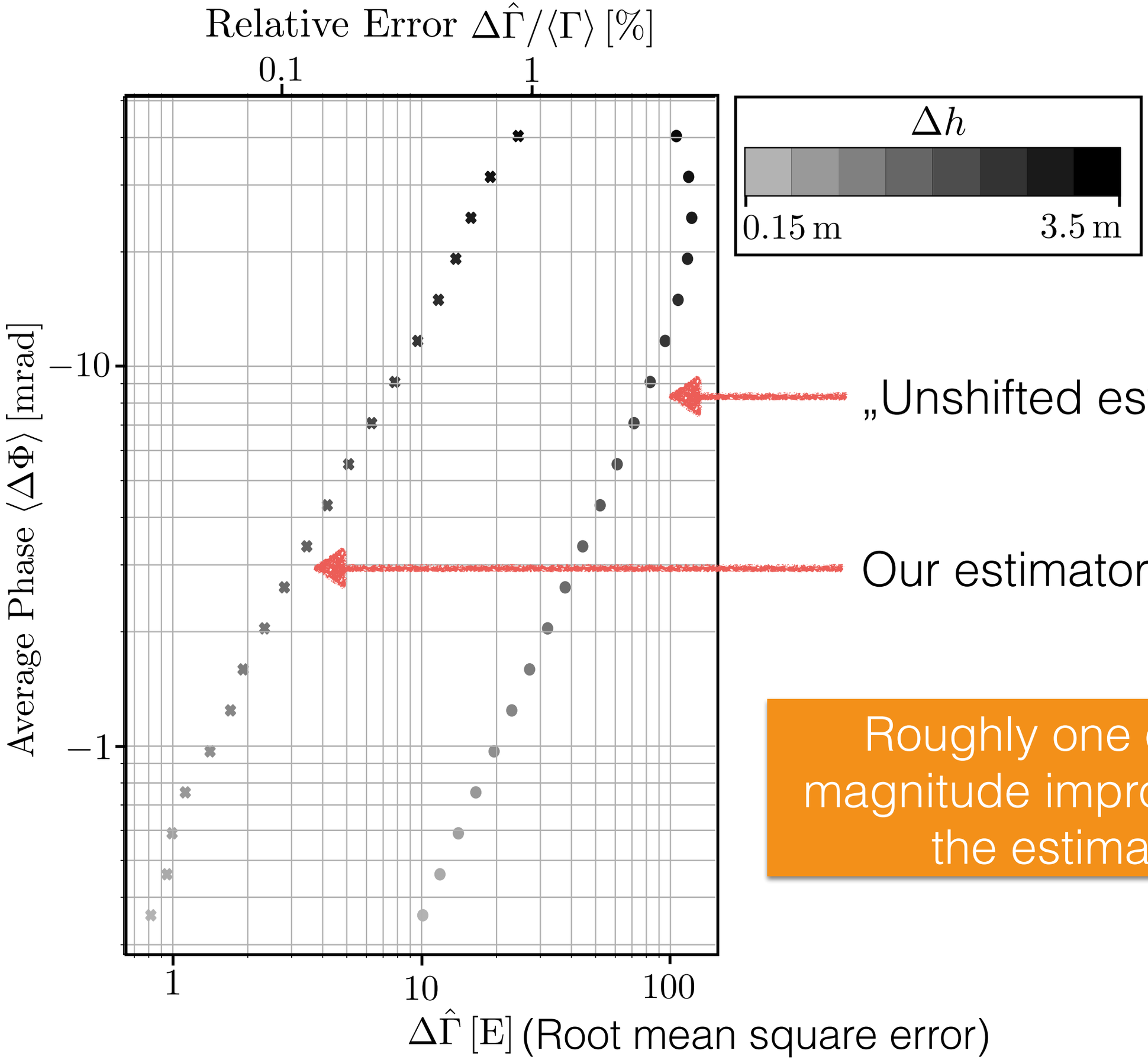

„Unshifted estimator“ $\frac{\Delta\Phi}{f}$

Our estimator $\hat{\Gamma}$

Roughly one order of magnitude improvement in the estimation!

Reference

Those findings have been published on the ArXiv

And the Python algorithm in the LUH Data Repository

Local Measurement Scheme of Gravitational Curvature using Atom Interferometers

Dataset for the paper "Local Measurement Scheme of Gravitational Curvature using Atom Interferometers".

All (numerical) figures are produced by this algorithm. The analytical phase calculation for the MZI, SDDI -- and ultimately the CGI -- are also done by this code for the case of an idealized gravitational potential.

An up-to-date version can be found in: https://gitlab.uni-hannover.de/michael.werner/vlbai-phase-shift-analysis/

Data and Resources

Local Measurement Scheme of Gravitational...
ZIP File of complete code with figures. File size: 188.6 KByte — Explore

README.md
README file. File size: 2.0 KByte — Explore

atom interferometry | gravitational field | gravitational gradient

Local Measurement Scheme of Gravitational Curvature using Atom Interferometers

Michael Werner*,[1] Ali Lezeik,[2] Dennis Schlippert,[2] Ernst M. Rasel,[2] Naceur Gaaloul,[2] and Klemens Hammerer[1]

[1]*Institut für Theoretische Physik, Leibniz Universität Hannover, Appelstraße 2, 30167 Hannover, Germany*
[2]*Institut für Quantenoptik, Leibniz Universität Hannover, Welfengarten 1, 30167 Hannover, Germany*

(Dated: October 7, 2024)

Light pulse atom interferometers (AIFs) are exquisite quantum probes of spatial inhomogeneity and gravitational curvature. Moreover, detailed measurement and calibration are necessary prerequisites for very-long-baseline atom interferometry (VLBAI). Here we present a method in which the differential signal of two co-located interferometers singles out a phase shift proportional to the curvature of the gravitational potential. The scale factor depends only on well controlled quantities, namely the photon wave number, the interferometer time and the atomic recoil, which allows the curvature to be accurately inferred from a measured phase. As a case study, we numerically simulate such a co-located gradiometric interferometer in the context of the Hannover VLBAI facility and prove the robustness of the phase shift in gravitational fields with complex spatial dependence. We define an estimator of the gravitational curvature for non-trivial gravitational fields and calculate the trade-off between signal strength and estimation accuracy with regard to spatial resolution. As a perspective, we discuss the case of a time-dependent gravitational field and corresponding measurement strategies.

I. INTRODUCTION

AIFs are high-precision instruments used in a wide variety of research fields. Their versatility includes tasks such as determining the fundamental constants [1–4], serving as quantum sensors to measure Earth's gravitational field [5–7], proposing measurements for gravitational wave detection [8–10], exploring fundamental physics and alternative gravitational models [11–14], and performing measurements related to time dilation and gravitational redshift [15–18]. In particular, their accuracy as sensors of gravitational fields and their gradients is becoming increasingly important for applications in civil engineering [19], inertial sensing [20] and geodesy [21–26].

AIFs are utilized to measure the gravitational field, there they provide information about the linear gravitational acceleration g along the atomic trajectory. This approach is highly accurate because the leading order phase shift $\Delta\Phi = gkT_R^2$ connects the desired value of g with the wave vector k and the interferometer time T_R, both of which are known with very high precision. For measuring the (constant) gravitational gradient, a gradiometric experimental setup is employed, involving a comparison of g-measurements from two spatially separated gravimeters, effectively interpolating the g values between their spatial positions. Such gradiometric experiments are theoretically limited by the measurement uncertainty of the phase shift and the uncertainty of the height difference between the two interferometers. Another way to extract knowledge about the gravity gradient is done using more elaborate AIF geometries [27]. In these cases, however, the phase shift depends non-linearly on the gravitational field, making an estimation more complicated.

State-of-the-art AIFs are being constructed with increasingly longer baselines [28–31] and more efficient large momentum transfer (LMT) techniques [32–34], extending beyond the region where the assumption of a constant gradient of the gravitational field remains valid. The transition to non-trivial gravitational curvature is not only a challenge for large baseline interferometers, but can also be seen as an opportunity for experiments with gravitational test masses. Deliberately

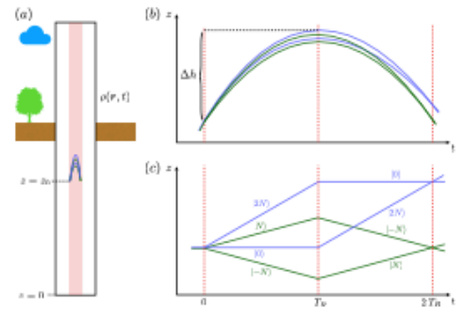

FIG. 1. Depiction of the co-located gradiometric interferometer (CGI) setup consisting of a SDDI (green) and a MZI (blue) in a gravitational field sourced by the mass density $\rho(\boldsymbol{r}, t)$. (a) Position of the CGI in a large baseline interferometry setup as as determined by the initial height z_0. CGI geometry shown in more detail (b) in the laboratory frame and (c) in the freely falling frame. $|N\rangle$ denotes a momentum eigenstate with N momentum quanta, as compared to the initial wave packet. The speed of light was set infinite for the laser pulses in this plot.

introduced non-trivial gravitational fields, which allow the measurement of phases along the atomic trajectory to probe this non-linearity, have been exploited in [35, 36] and led to the proposed gravitational Aharonov-Bohm effect [37]. Measuring anomalies in the gravitational gradient is also used to detect inhomogeneities in the gravitational field [19] and will become evermore important for civil engineering and quantum metrology. Resolving a spatially varying gravity gradient to high accuracy with a gradiometric AIF setup is, however, equivalent to comparing g-measurements in close proximity. This procedure is therefore increasingly error prone, because of the relative uncertainty in the position of the atomic ensembles, compared to the separation of the two constituent AIFs.

In this analysis, we introduce a novel geometry for AIFs that is exclusively sensitive to the gravitational curvature, that is,

Outlook / Summary

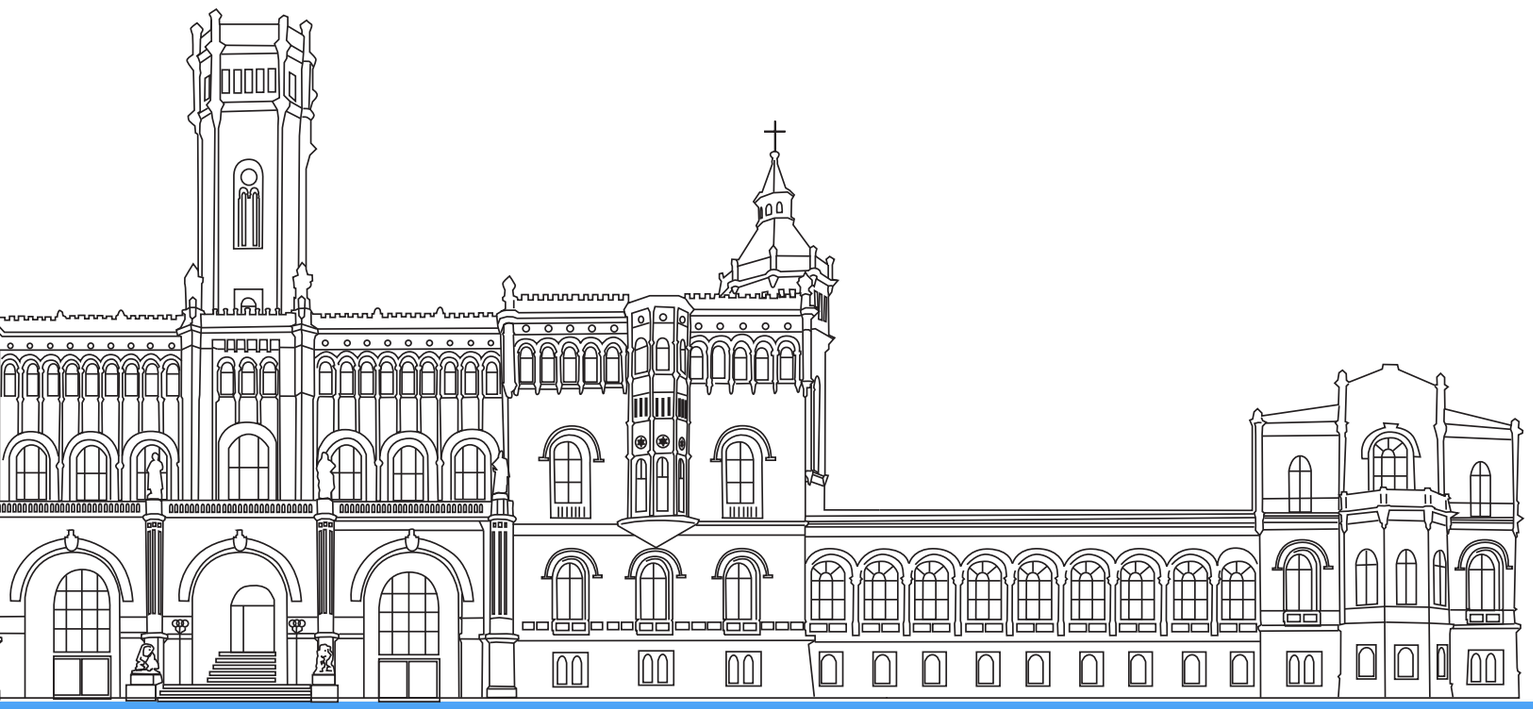

Outlook / Summary

- We presented an open source Python algorithm to quickly calculate phase shifts in (pretty much) arbitrary geometries.

Want to include even more effects: Clock interferometry, Mitigation schemes, Coriolis effect, …(Partially done in the transition from the #1 to #2 algorithm)

- Included first order GR effects into the description.

Search for interesting geometries that might single out GR-related phases (for next Gen AIFs, i.e. ~100m baseline)

- We introduced a novel AIF geometry — the „CGI“ — that gives information about gravitational curvature.

Possibly useful in civil engineering and geodesy?

Thank you for listening!
Any questions?

And also thanks to those people

Hammerer group

Gaaloul group (T-SQUAD)

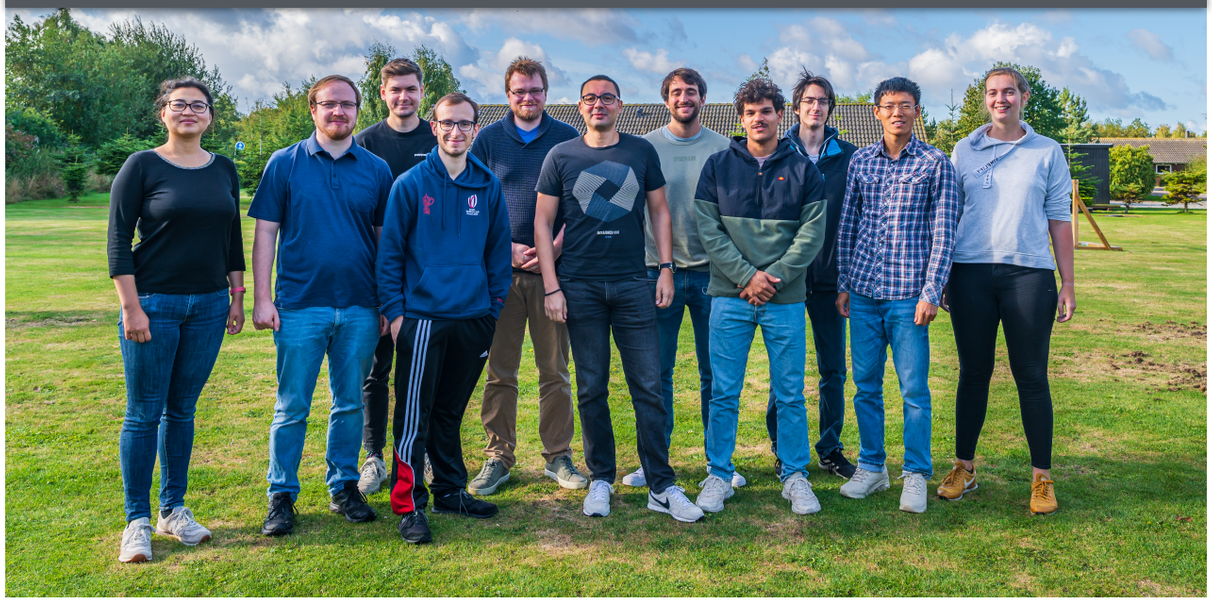

Other Co-Authors: Ali Lezeik, Philip Schwartz, Domenico Giulini, Dennis Schlippert, and Ernst M. Rasel

Quick links:

PPN paper:

Curvature paper:

We looked @ this code

PPN algorithm:

Curv. algorithm:

Backup Slides

Maxwell's equations: Geometric Coulomb gauge

We can define a flat Laplace operator via

$$\Delta_{\text{flat}} = \delta^{ij}\partial_i\partial_j = \partial_x^2 + \partial_y^2 + \partial_z^2$$

And obtain the wave equations

$$\overline{\phi}(z) = \phi(z) - \phi_0$$

$$\Delta_{\text{flat}} A_\nu = \left(1 - 2(\gamma+1)\frac{\overline{\phi}}{c^2}\right)\left(\partial_0^2 A_\nu + \Gamma^z{}_{00}\left(\partial_\nu A_z - \partial_z A_\nu\right) - \Gamma^\sigma{}_{0\nu}\partial_0 A_\sigma + \Gamma^\sigma{}_{0\nu}\partial_\sigma A_0 - \partial_\nu\partial_0 A_0\right)$$

$$+ \sum_{i=1}^{3}\left(\Gamma^\sigma{}_{ii}\partial_\sigma A_\nu + (\partial_\nu\Gamma^\sigma{}_{ii})A_\sigma + \Gamma^\sigma{}_{i\nu}\partial_i A_\sigma - \Gamma^\sigma{}_{i\nu}\partial_\sigma A_i\right) + \mathcal{O}(c^{-4})$$

Christoffel symbols
(need to be calculated)

Maxwell's equations: Geometric Coulomb gauge

$$\Delta_{\text{flat}} A_0 = (\gamma+1)\frac{\partial_z\overline{\phi}}{c^2}\partial_z A_0 - \frac{\partial_z\overline{\phi}}{c^2}\partial_0 A_z + O(c^{-4}),$$

$$\Delta_{\text{flat}} A_x = \left(1 - 2(\gamma+1)\frac{\overline{\phi}}{c^2}\right)\partial_0^2 A_x + \gamma\frac{\partial_z\overline{\phi}}{c^2}\partial_z A_x + (2\gamma+1)\frac{\partial_z\overline{\phi}}{c^2}\left(\partial_x A_z - \partial_z A_x\right)$$
$$- \left(1 - 2(\gamma+1)\frac{\partial_z\overline{\phi}}{c^2}\right)\partial_x\partial_0 A_0 + O(c^{-4}),$$

$$\Delta_{\text{flat}} A_y = \left(1 - 2(\gamma+1)\frac{\overline{\phi}}{c^2}\right)\partial_0^2 A_y + \gamma\frac{\partial_z\phi}{c^2}\partial_z A_y + (2\gamma+1)\frac{\partial_z\phi}{c^2}\left(\partial_y A_z - \partial_z A_y\right)$$
$$- \left(1 - 2(\gamma+1)\frac{\partial_z\overline{\phi}}{c^2}\right)\partial_y\partial_0 A_0 + O(c^{-4}),$$

$$\Delta_{\text{flat}} A_z = \left(1 - 2(\gamma+1)\frac{\overline{\phi}}{c^2}\right)\partial_0^2 A_z + \gamma\frac{\partial_z\overline{\phi}}{c^2}\partial_z A_z + \gamma\frac{\partial_z^2\overline{\phi}}{c^2}A_z$$
$$- \left(1 - 2(\gamma+1)\frac{\partial_z\overline{\phi}}{c^2}\right)\partial_z\partial_0 A_0 + O(c^{-4}).$$

Maxwell's equations: Leading order

Since we know $k_\mu = \nabla_\mu \Phi = \partial_\mu \Phi$

one obtains a **gravitationally altered phase** of

$$\Phi(z,t) = \Phi_0 + k_0 ct \pm \left(1 - \frac{\gamma+1}{2}\frac{gz}{c^2}\right) k_0 z + \mathcal{O}(\Gamma c^{-2})$$

Additional height dependence of the phase!

Phase shift results

We can now extend the previous list of phase shifts:

Phases in units of ω_C							
#	Order	Proportionality	SRBI	SDDI	ARBI	α	Origin
44	$O(3)$	$\mathcal{G}_0\mathcal{G}_{1,\mathrm{R}}\mathcal{R}_\mathrm{R}$	$2(\beta-1)(T_B+T_R)$	$4(\beta-1)(T_B+T_R)$	$2(\beta-1)(T_B+T_R)$	2	Post-Newtonian
45	$O(4)$	$\mathcal{R}_\mathrm{R}\mathcal{G}_{1,\mathrm{R}}\mathcal{V}_0\mathcal{R}_\mathrm{B}$	$-\frac{13\gamma+20}{2}T_B-\frac{20\gamma+41}{2}T_R$	$-(13\gamma+20)T_B-(20\gamma+41)T_R$	$-\frac{13\gamma+20}{2}T_B-\frac{20\gamma+41}{2}T_R$	2	Post-Newtonian
46		$\mathcal{R}_\mathrm{R}\mathcal{G}_{1,\mathrm{R}}\mathcal{V}_0^2$	$-\frac{10\gamma+11}{2}T_B-\frac{8\gamma+11}{2}T_R$	$-(10\gamma+11)T_B-(8\gamma+11)T_R$	$-\frac{10\gamma+11}{2}T_B-\frac{8\gamma+11}{2}T_R$	2	
47		$\mathcal{R}_\mathrm{R}\mathcal{G}_{1,\mathrm{R}}^2\mathcal{V}_0$	$\frac{8\beta+48\gamma+51}{2}T_B+\frac{4\beta+30\gamma+38}{2}T_R$	$(8\beta+48\gamma+51)T_B+(4\beta+30\gamma+38)T_R$	$\frac{8\beta+48\gamma+51}{2}T_B+\frac{4\beta+30\gamma+38}{2}T_R$	3	
48		$\mathcal{R}_\mathrm{R}\mathcal{G}_{1,\mathrm{R}}^2\mathcal{R}_\mathrm{B}$	$\frac{12\beta+165\gamma+264}{12}T_B+\frac{112\gamma+242}{12}T_R$	$\frac{12\beta+165\gamma+264}{6}T_B+\frac{112\gamma+242}{6}T_R$	$\frac{12\beta+165\gamma+264}{12}T_B+\frac{112\gamma+242}{12}T_R$	3	
49		$\mathcal{R}_\mathrm{R}\mathcal{G}_{1,\mathrm{R}}^3$	$-\frac{36\beta+220\gamma+278}{12}T_B-\frac{4\beta+93\gamma+151}{12}T_R$	$-\frac{36\beta+220\gamma+278}{6}T_B-\frac{4\beta+93\gamma+151}{6}T_R$	$-\frac{36\beta+220\gamma+278}{12}T_B-\frac{4\beta+93\gamma+151}{12}T_R$	4	
50		$\mathcal{R}_\mathrm{R}\mathcal{G}_{1,\mathrm{R}}\mathcal{R}_\mathrm{B}^2$	$-\frac{8\gamma+17}{4}T_B-\frac{10\gamma+35}{4}T_R$	$-\frac{8\gamma+17}{2}T_B-\frac{10\gamma+35}{2}T_R$	$-\frac{8\gamma+17}{4}T_B-\frac{10\gamma+35}{4}T_R$	2	
51		$\mathcal{R}_\mathrm{R}\mathcal{G}_{1,\mathrm{R}}\mathcal{G}_{1,\mathrm{B}}^2$	$\frac{\beta-43\gamma-52}{24}T_B$	$\frac{\beta-43\gamma-52}{12}T_B$	$\frac{\beta-43\gamma-52}{24}T_B$	4	
52		$\mathcal{R}_\mathrm{R}\mathcal{G}_{1,\mathrm{R}}^2\mathcal{G}_{1,\mathrm{B}}$	$-\frac{6\beta+44\gamma+51}{4}T_B$	$-\frac{6\beta+44\gamma+51}{2}T_B$	$-\frac{6\beta+44\gamma+51}{4}T_B$	4	
53		$\mathcal{R}_\mathrm{R}\mathcal{G}_{1,\mathrm{R}}\mathcal{G}_{1,\mathrm{B}}\mathcal{V}_0$	$\frac{\beta+13\gamma+13}{2}T_B$	$(\beta+13\gamma+13)T_B$	$\frac{\beta+13\gamma+13}{2}T_B$	3	
54		$\mathcal{R}_\mathrm{R}\mathcal{G}_{1,\mathrm{R}}\mathcal{G}_{1,\mathrm{B}}\mathcal{R}_\mathrm{B}$	$\frac{8\gamma+11}{2}T_B$	$(8\gamma+11)T_B$	$\frac{8\gamma+11}{2}T_B$	3	
55		$\mathcal{R}_\mathrm{R}\mathcal{G}_0\mathcal{G}_{1,\mathrm{R}}\mathcal{G}_{2,\mathrm{R}}$	$\frac{57\beta-57}{3}T_B+\frac{25\beta-25}{3}T_R$	$2\frac{57\beta-57}{3}T_B+2\frac{25\beta-25}{3}T_R$	$\frac{57\beta-57}{3}T_B+\frac{25\beta-25}{3}T_R$	4	
⋮		⋮	⋮	⋮	⋮	⋮	
56		$\mathcal{G}_{3,\mathrm{R}}\mathcal{R}_\mathrm{R}\mathcal{V}_0^2$	$\frac{T_B^3+12T_B^2T_R+8T_R^2(3T_B+T_R)}{8T_R^2}$	$\frac{T_B^3+12T_B^2T_R+8T_R^2(3T_B+T_R)}{4T_R^2}$	$\frac{T_B^3+12T_B^2T_R+8T_R^2(3T_B+T_R)}{8T_R^2}$	4	3rd order grav. potential
57		$\mathcal{G}_{3,\mathrm{R}}\mathcal{R}_\mathrm{R}^2\mathcal{V}_0$	$\frac{T_B^2+4T_R^2(2T_B+T_R)}{4T_R}$	0	$\frac{T_B^2+4T_R^2(2T_B+T_R)}{4T_R}$	4	
⋮		⋮	⋮	⋮	⋮	⋮	

Backup: Coriolis & Centrifugal effects

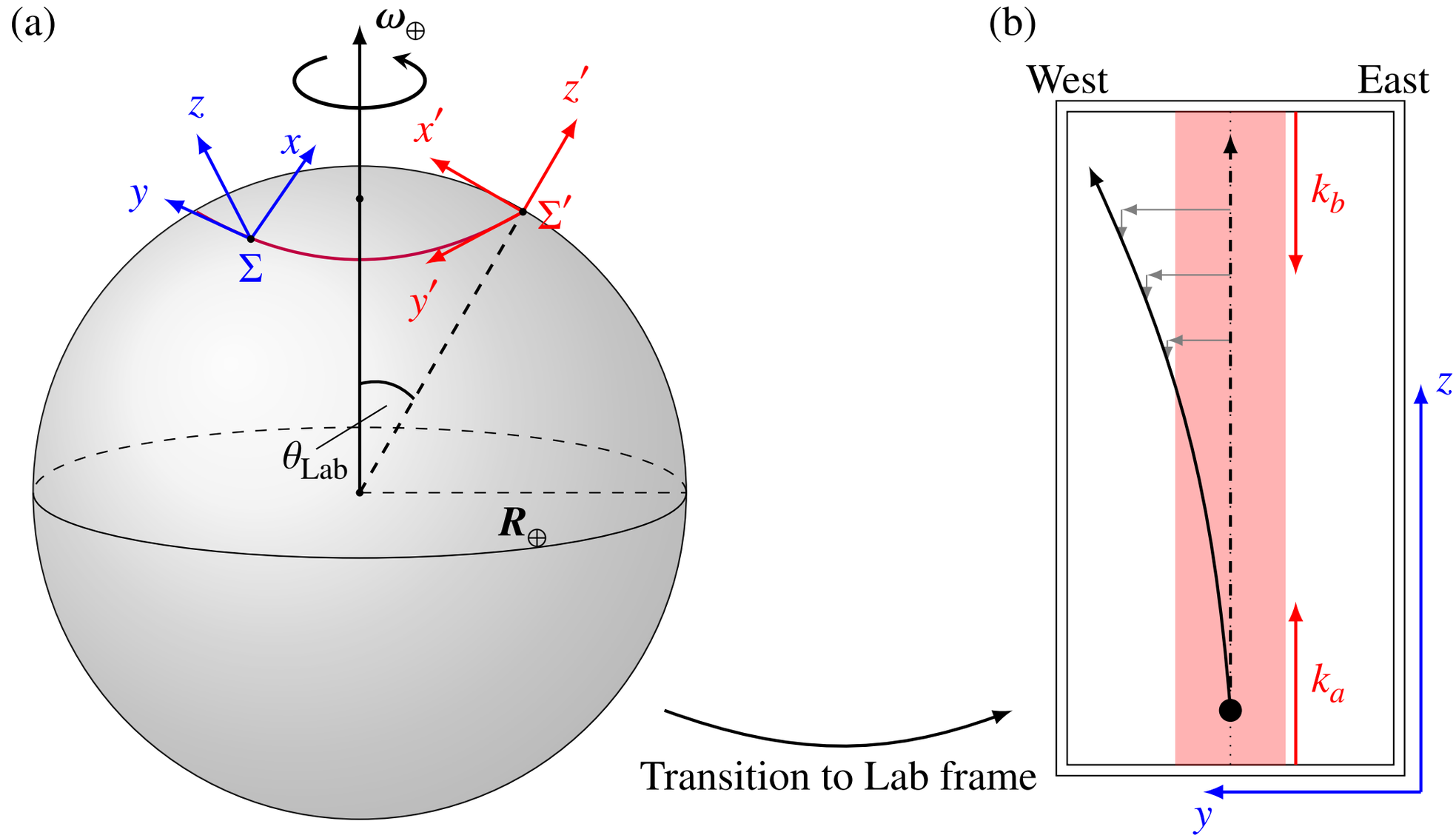

$$L(\boldsymbol{r}, \dot{\boldsymbol{r}}) = \frac{m}{2}\dot{\boldsymbol{r}}^2 + \underbrace{m\dot{\boldsymbol{r}} \cdot (\boldsymbol{\omega}_\oplus \times \boldsymbol{r})}_{\text{Coriolis}} + \underbrace{\frac{m}{2}(\omega_\oplus \times \boldsymbol{r})^2}_{\text{Centrifugal}} - m\phi(\boldsymbol{r}),$$

Backup: Coriolis & Centrifugal effects

$$L(\boldsymbol{r}, \dot{\boldsymbol{r}}) = \frac{m}{2}\dot{\boldsymbol{r}}^2 + \frac{m}{2} r^2 \dot{\varphi}^2 \sin^2(\theta) + m\omega_{\oplus} r^2 - m\phi(\boldsymbol{r})$$

Lagrangian is quadratic in its arguments.

Analytical solution can be found!

$$\hbar\Delta\Phi_{\mathrm{Prop}}\ (\boldsymbol{r}_b, t_b; \boldsymbol{r}_a, t_a) = S_{\mathrm{z}}\left(z_b, t_b; z_a, t_a\right) + S_{\mathrm{xy}}\left(x_b, y_b, t_b; x_a, y_a, t_a\right)$$

Discussed before

New transversal motion

$$S_{\mathrm{xy}}\left(x_b, y_b, t_b; x_a, y_a, t_a\right) = \frac{m}{2\left(t_b - t_a\right)}\left[\left(x_b - x_a\right)^2 + \left(y_b - y_a\right)^2\right] + m\omega_{\mathrm{eff}}\left(x_a y_b - x_b y_a\right)$$

$$\text{with}\ \ \omega_{\mathrm{eff}} = \omega_{\oplus}\sin(\theta_{\mathrm{Lab}})$$

Backup: Relativistic Atom-Light Interaction

Consider the next order correction to the electric dipole operator:

$$\hat{H}_{\text{A-L}} = \underbrace{-\hat{\boldsymbol{d}} \cdot \boldsymbol{E}(\hat{Z})}_{\text{Electric dipole}} + \underbrace{\frac{1}{2m}\left[\hat{P}\Big(\hat{\boldsymbol{d}} \times \boldsymbol{B}(\hat{Z})\Big)_z + \text{h.c.}\right]}_{\text{Röntgen term}}$$

The electromagnetic fields are given by their classical solutions:

Electric/Magnetic fields

$$\boldsymbol{E}_i(\hat{Z}, t) = \mathcal{E}_i(t) e^{\mathrm{i}\Phi_i(\hat{Z},t)}$$

$$\boldsymbol{B}_i(\hat{Z}, t) = \pm\mathcal{B}_i(t) e^{\mathrm{i}\Phi_i(\hat{Z},t)}$$

Amplitudes

$$\mathcal{E}_i(t) = -\mathrm{i}\omega_i \mathcal{A}_i(t) - \dot{\mathcal{A}}_i(t)$$

$$\mathcal{B}_i(t) = \mathrm{i}k_i \boldsymbol{e}_z \times \mathcal{A}_i(t)$$

Backup: Relativistic Atom-Light Interaction

First, we transform into the interaction picture w.r.t. the internal Hamiltonian

$$\hat{\boldsymbol{d}}(t) = e^{\mathrm{i}\hat{H}_\mathrm{I}t/\hbar}\hat{\boldsymbol{d}}e^{-\mathrm{i}\hat{H}_\mathrm{I}t/\hbar} = \boldsymbol{d}_\mathrm{eg}\left|e\right\rangle\!\left\langle g\right| e^{\mathrm{i}\omega_\mathrm{eg}t}$$

$$\hat{H} = \hat{H}_\mathrm{COM} + \sum_{i=a,b}\frac{\hbar\Omega_i(\hat{Z},\hat{P},t)}{2}\left|e\right\rangle\!\left\langle g\right| e^{\mathrm{i}\left(\pm k_i(\hat{Z})\hat{Z}-(\omega_i-\omega_\mathrm{eg})t\right)}$$

Backup: Stationary Spacetime

Spacetime metric of a rotating mass

$$g_{\mu\nu} = \begin{pmatrix} -1 - 2\frac{\phi(\boldsymbol{r})}{c^2} - 2\beta\frac{\phi(\boldsymbol{r})^2}{c^4} + O(c^{-6}) & -\frac{4+4\gamma+\alpha_1}{2c^3}\boldsymbol{V}(\boldsymbol{r})^T + O(c^{-5}) \\ -\frac{4+4\gamma+\alpha_1}{2c^3}\boldsymbol{V}(\boldsymbol{r}) + O(c^{-5}) & \left(1 - 2\gamma\frac{\phi(\boldsymbol{r})}{c^2}\right)\mathbb{1}_3 + O(c^{-4}) \end{pmatrix}$$

From this we can calculate the motional Lagrangian

$$L^{\mathrm{Rot}}(\boldsymbol{r}, \dot{\boldsymbol{r}}) = L(\boldsymbol{r}, \dot{\boldsymbol{r}}) + m\dot{\boldsymbol{r}} \cdot (\boldsymbol{\omega}_\oplus \times \boldsymbol{r}) + \frac{m}{2}(\boldsymbol{\omega}_\oplus \times \boldsymbol{r})^2 - \frac{4 + 4\gamma + \alpha_1}{4}\frac{mG}{r^3 c^2}(\boldsymbol{r} \times \dot{\boldsymbol{r}}) \cdot \boldsymbol{J}_\oplus + O\left(c^{-4}\right)$$

Coriolis Centrifugal Frame-Dragging

Backup: Experimental realization of 4-way beam splitter

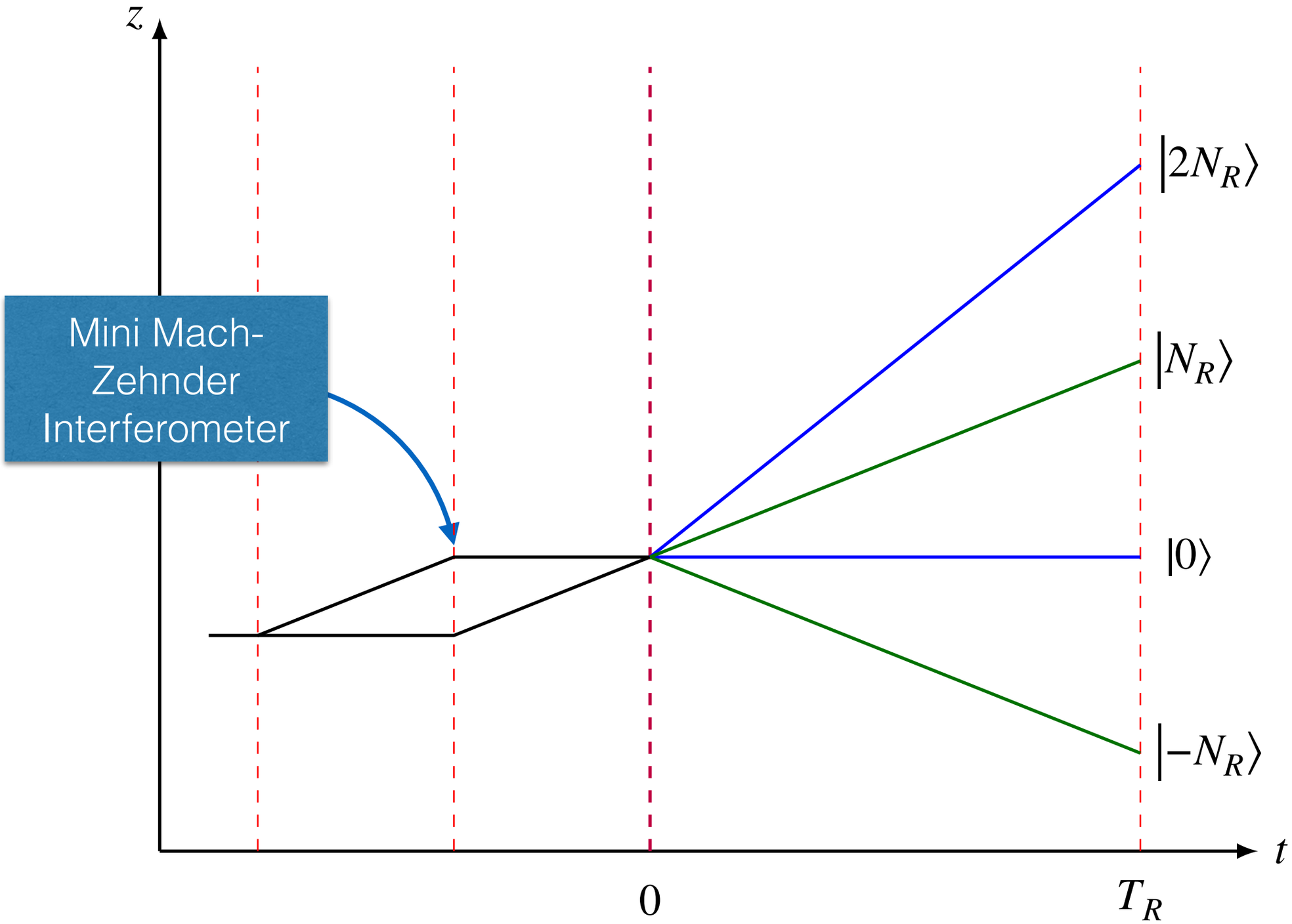

Backup: Doppler effect

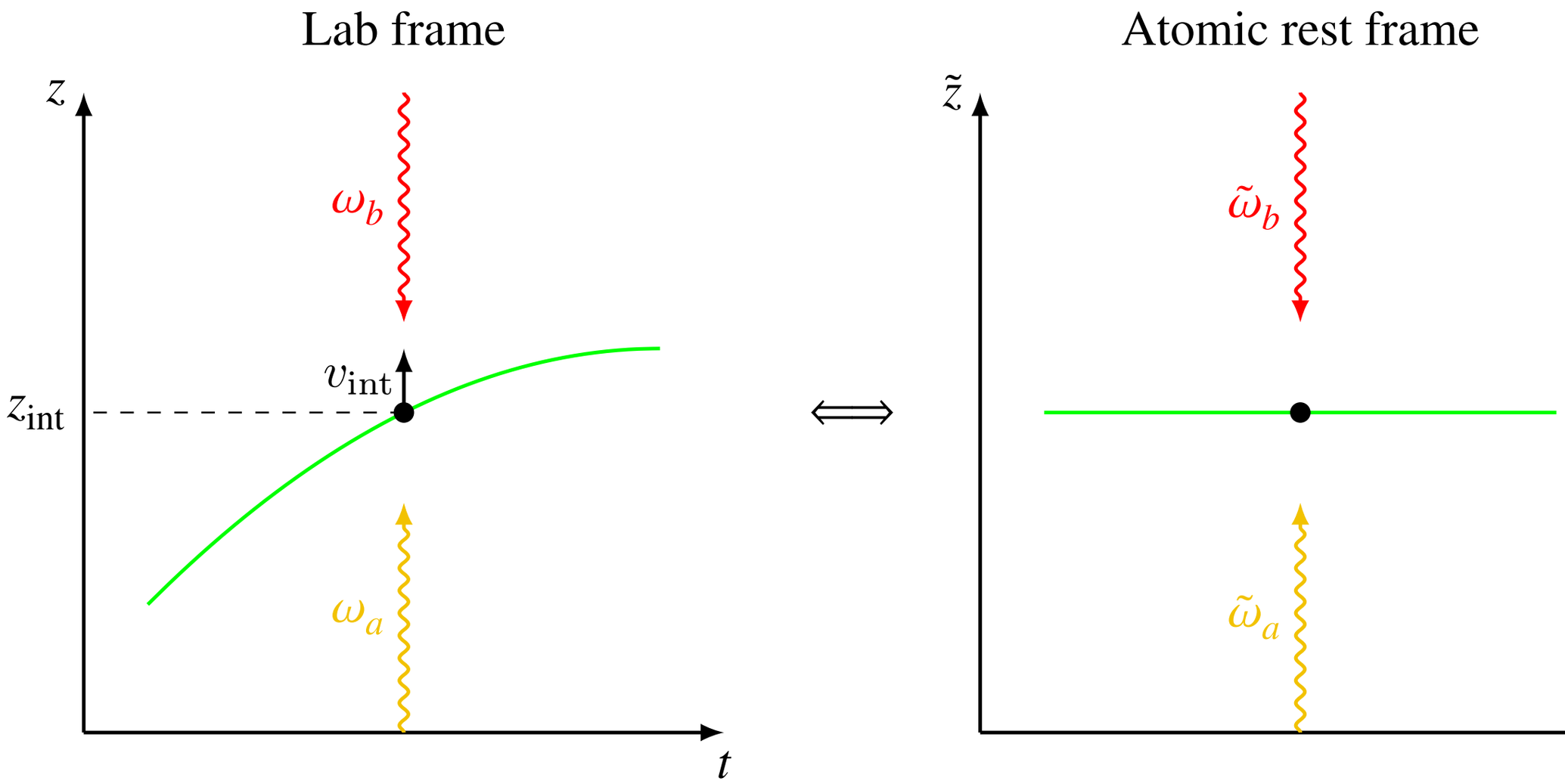

$$\tilde{\omega}_a = \left(1 - \frac{v_{\rm int}}{c} + \frac{v_{\rm int}^2}{c^2}\right)\omega_a, \qquad \tilde{\omega}_b = \left(1 + \frac{v_{\rm int}}{c} + \frac{v_{\rm int}^2}{c^2}\right)\omega_b$$

Backup: Gradient mitigation

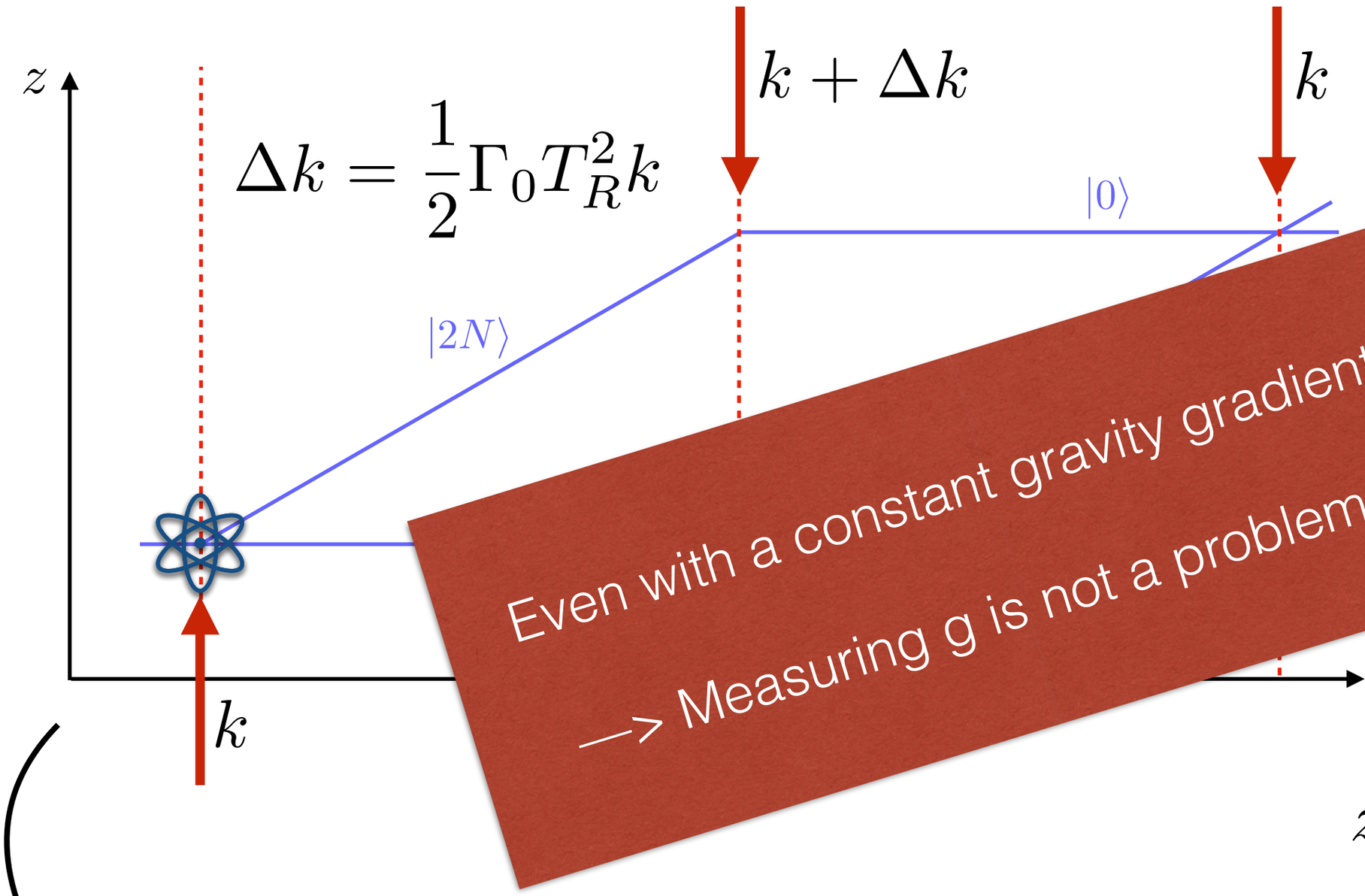

Even with a constant gravity gradient

—> Measuring g is not a problem!

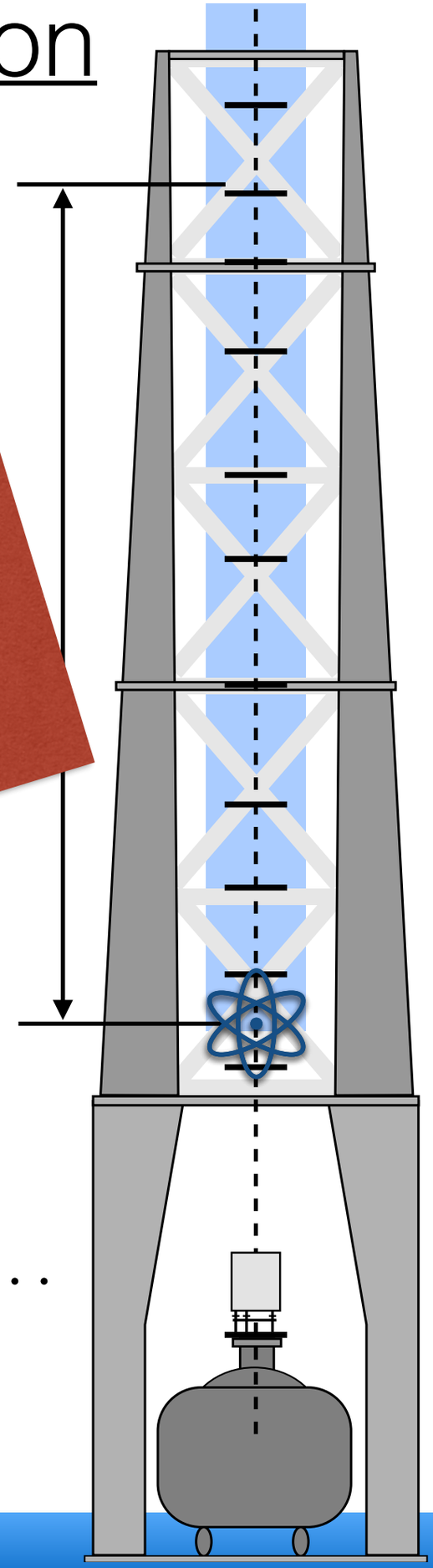

$$\Delta\Phi = 2NgkT_R^2 + \Gamma_0 Nk\underbrace{\left(2z_0 T_R^2 + 2v_0 T_R^3 - \frac{7}{6}gT_R^4\right)}_{\text{„Unwanted“ additional phases}} + \dots$$

Backup: Geopotential model

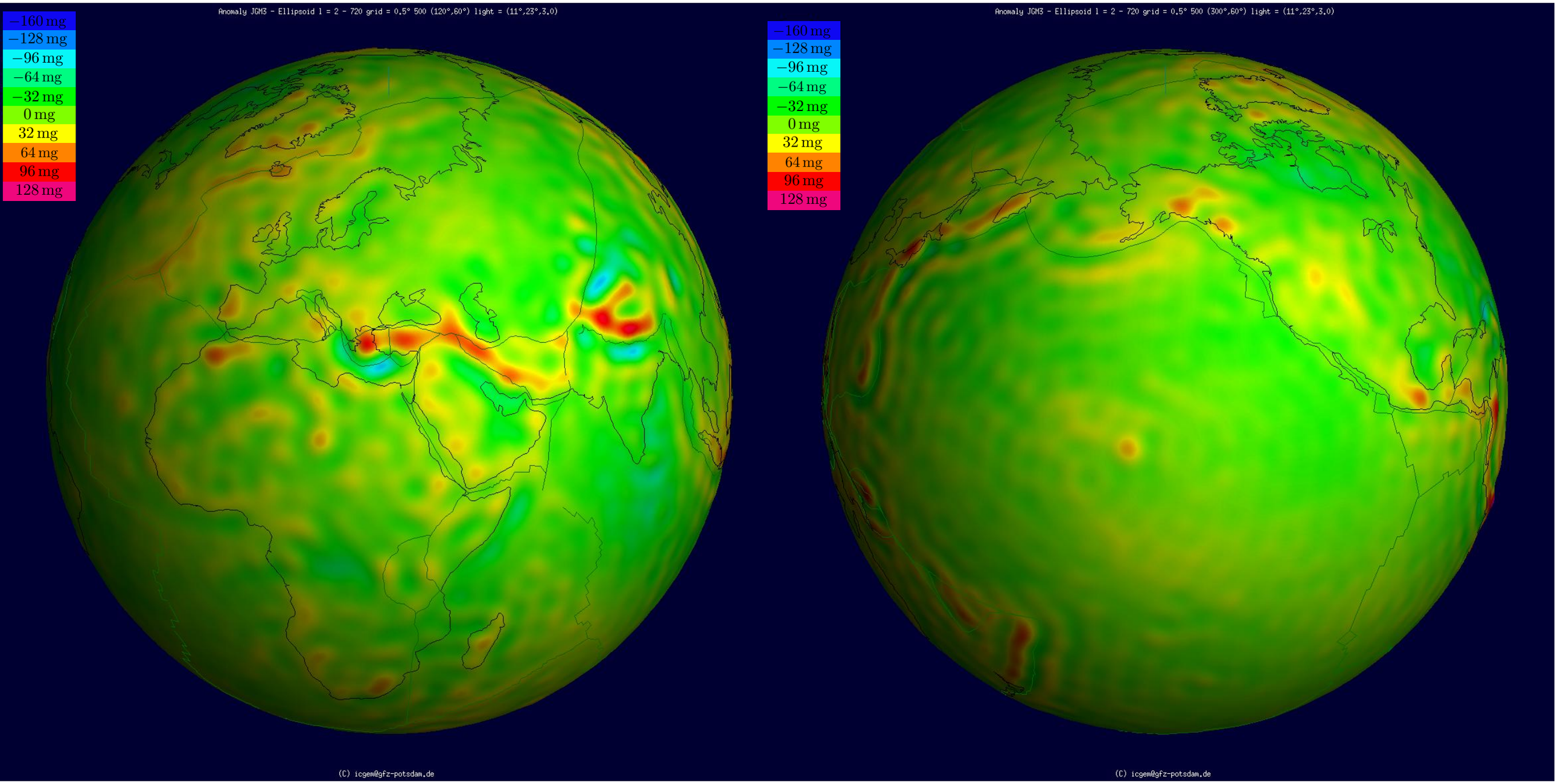

Figure from ICGEM and adapted for better readability.

Backup: Geopotential model

We can perform a multipole expansion of the gravitational potential of the form:

$$\phi(r,\theta,\varphi) = -\frac{GM_\oplus}{r} + \sum_{l=2}^{\infty} Z_l(r,\theta) + \sum_{n=2}^{\infty}\sum_{m=1}^{n} T_{n,m}(r,\theta,\varphi)$$

With „zonal“ and „tesseral“ contributions:

$$Z_l(r,\theta) = \frac{J_l P_l^0(\sin(\theta))}{r^{l+1}},$$

$$T_{n,m}(r,\theta,\varphi) = P_n^m(\sin(\theta))\frac{C_n^m\cos(m\varphi) + S_n^m\sin(m\varphi)}{r^{n+1}}$$

A list of the J’s, C’s and S’s can be found in geodata catalogs.

Backup: Geopotential model

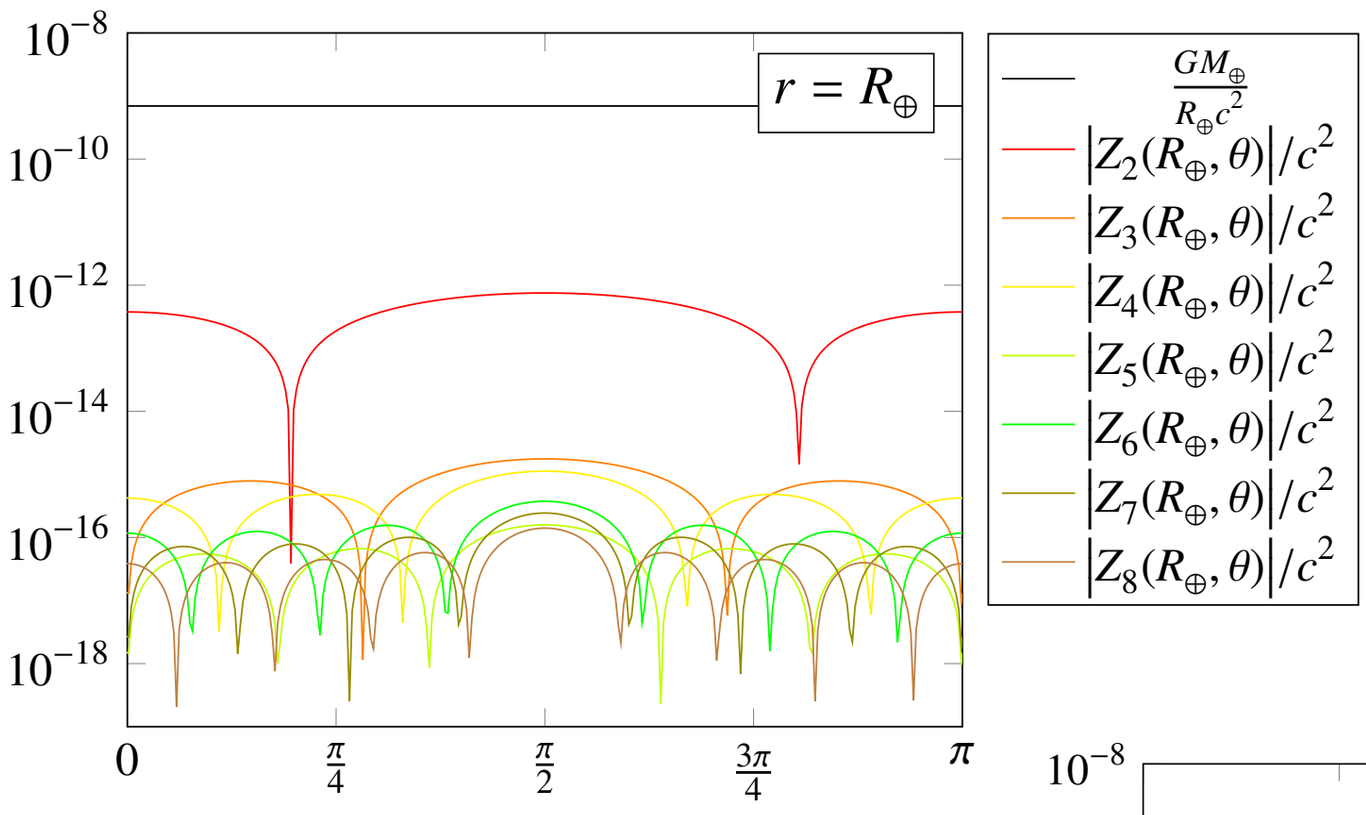

Zonal contributions

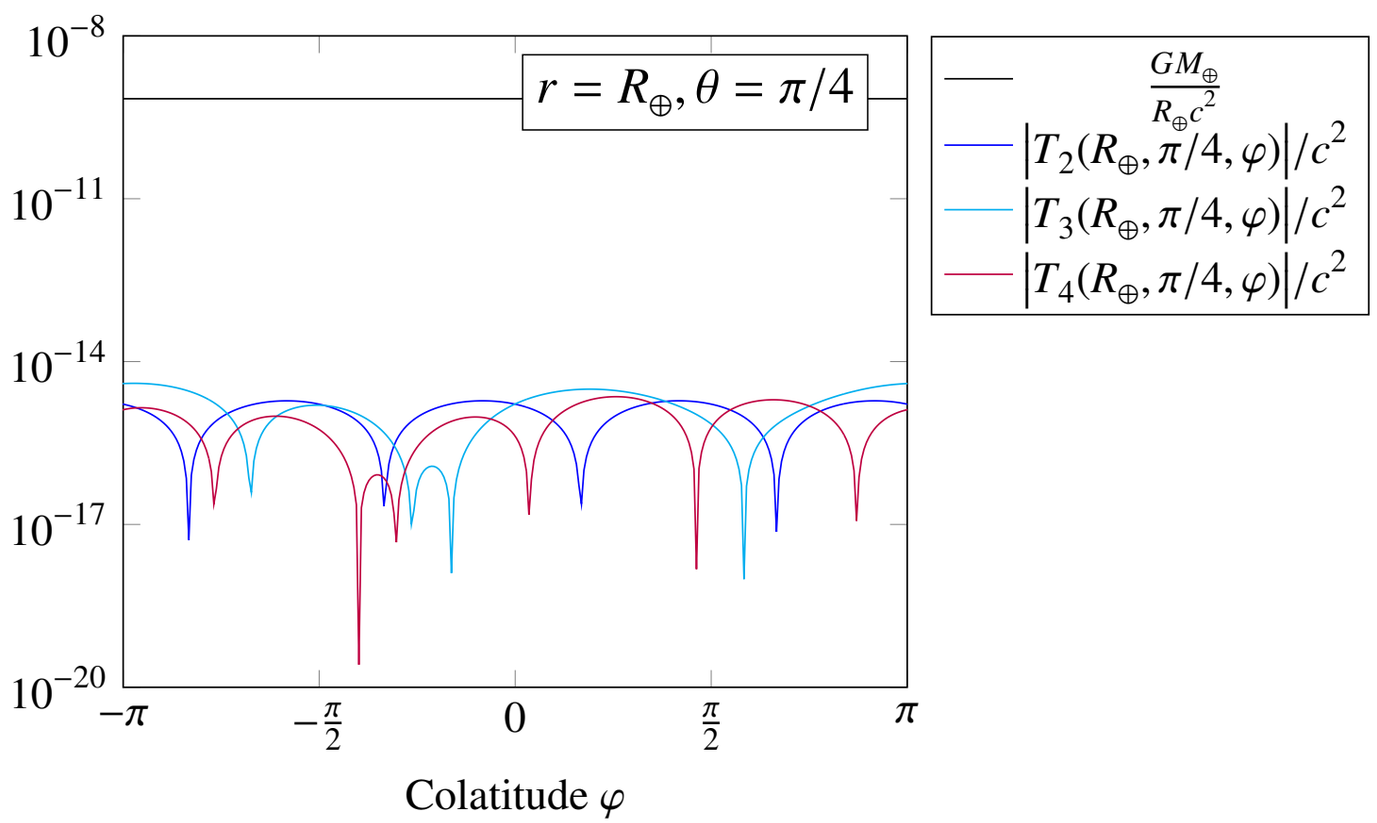

Tesseral contributions

Backup: Relativistic Atom-Light Interaction

$$k_i(z) = \left(1 - (\gamma + 1)\frac{gz}{c^2}\right)k_i + \mathcal{O}(\Gamma_0 c^{-2}, c^{-4})$$

$$\phi_i(z) = \left(1 - \frac{\gamma + 1}{2}\frac{gz}{c^2}\right)k_i z + \omega_i t + \mathcal{O}(\Gamma_0 c^{-2}, c^{-4})$$

Two-Photon process: Depending direction of the momentum kick

$$\Phi_{\mathrm{L}}(z) = \pm\left(1 + \frac{\gamma + 1}{2}\frac{gz}{c^2}\right)k_{\mathrm{R}} z + \Delta\Phi_{\mathrm{FSL}} + \mathcal{O}(\Gamma_0 c^{-2})$$

Backup: Gravitational Redshift

How does this relate to the gravitational redshift?
Consider a resting observer at a height z with four velocity

$$u^\mu(z) = \alpha(z) \begin{pmatrix} c \\ 0 \end{pmatrix}$$

Since four velocities always satisfy $u_\mu(z)u^\mu(z) = -c^2$ we have

$$u^\mu(z) = \left(1 - \frac{\overline{\phi}(z)}{c^2} + \mathcal{O}(c^{-4})\right) \begin{pmatrix} c \\ 0 \end{pmatrix}$$

The observer then measures the following frequency:

$$\omega(z) = -k_\mu(z)u^\mu(z) = -\left(1 - \frac{\overline{\phi}(z)}{c^2} + \mathcal{O}(c^{-4})\right) ck_0$$

Backup: Raman diffraction

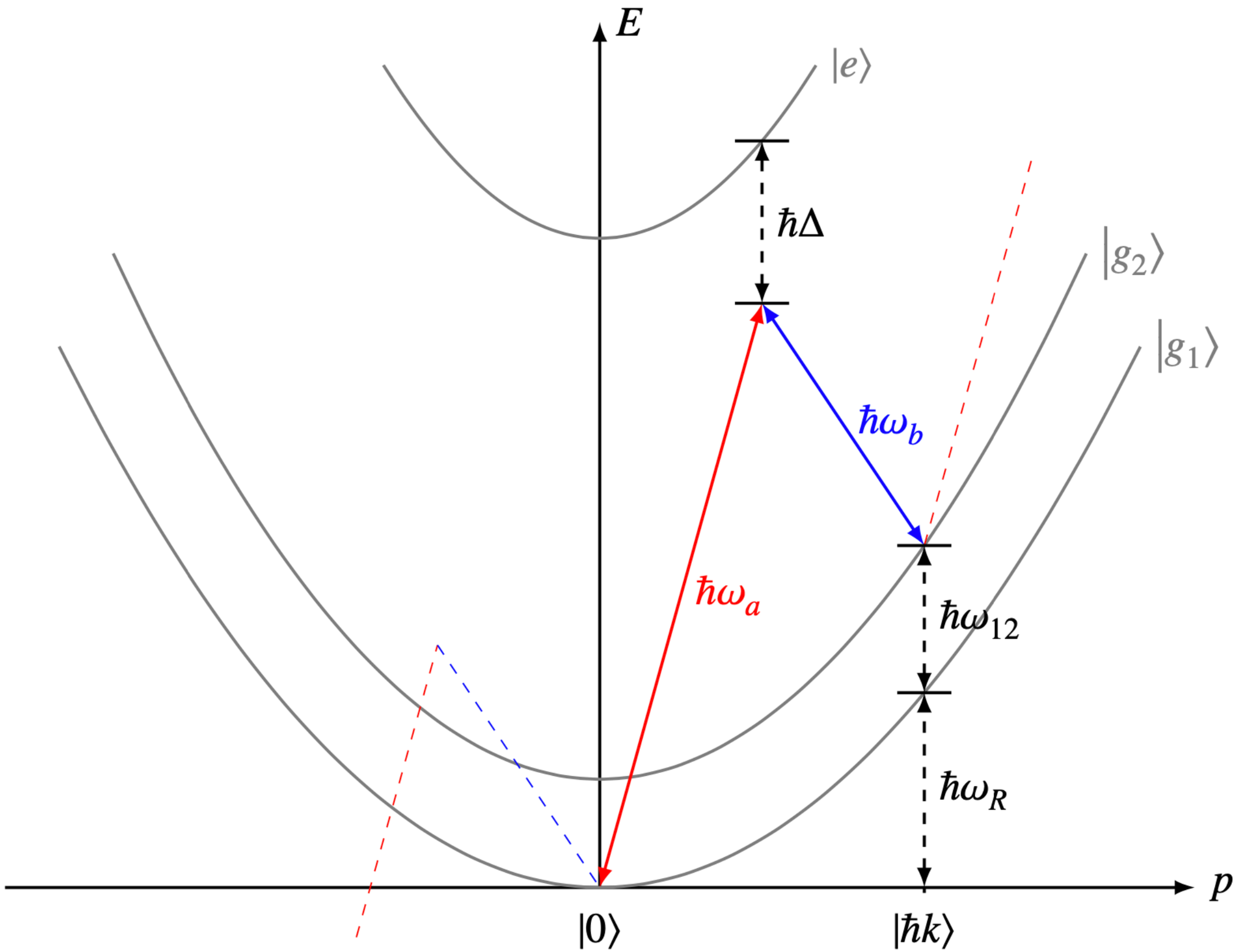

Backup: Single Photon Transition

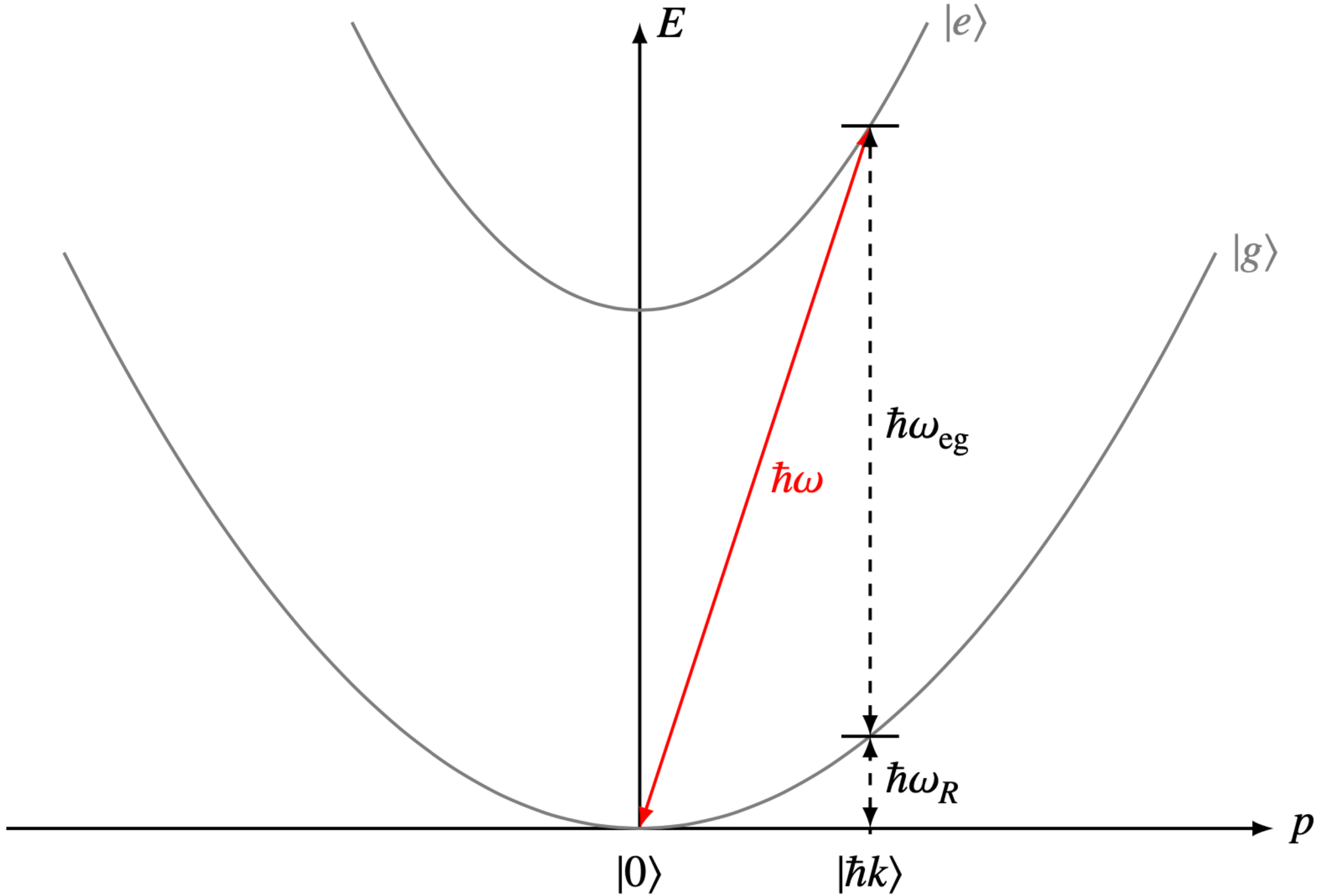

Backup: AIFs for GW detection

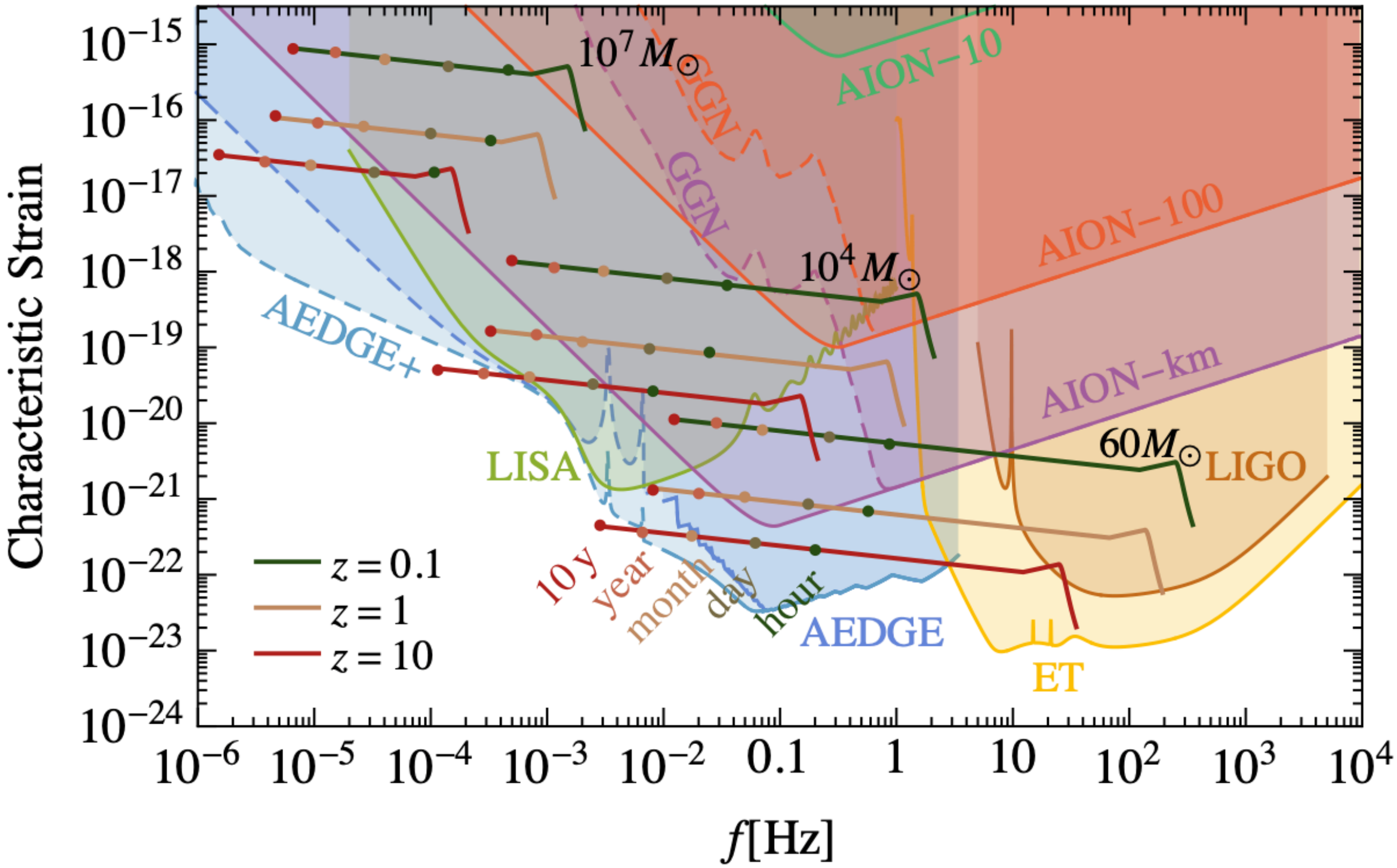

From Abdalla et al. „Terrestrial Very-Long-Baseline Atom Interferometry: Summary of the Second Workshop“

Backup: Full set of dimensionless parameters

Parameter	Definition	Magnitude for 10 m baseline AIF	
		$i = R$ (Bragg)	$i = B$ (Bloch)
$\mathcal{Z}_0$	$\frac{z_0}{cT_R}$	0	
$\mathcal{V}_0$	$\frac{v_0}{c}$	4.3×10^{-8}	
$\mathcal{F}_\mathrm{R}$	$\frac{\hbar\omega_R}{mc^2}$	8.1×10^{-20}	
$\mathcal{G}_0$	$\frac{\phi_0}{c^2}$	7×10^{-10}	
$\mathcal{Z}_L$	$\frac{z_L}{cT_R}$	2.6×10^{-9}	
$\mathcal{Z}_U$	$\frac{z_U}{cT_R}$	2.8×10^{-8}	
$\mathcal{H}$	$\frac{z_U - z_L}{cT_R}$	3.1×10^{-8}	
$\mathcal{G}_{1,i}$	$\frac{gT_i}{c}$	4.2×10^{-8}	1.3×10^{-8}
$\mathcal{G}_{2,i}$	ΓT_i^2	5.2×10^{-6}	4.9×10^{-7}
$\mathcal{G}_{3,i}$	$\Lambda c T_i^3$	4.8×10^{-4}	1.4×10^{-5}
$\mathcal{R}_i$	$\frac{\hbar k_i}{mc}$	3.9×10^{-11}	1.2×10^{-9}

→ Constant potential offset

→ Finite speed of light

→ Third order grav. potential

Backup: Gradiometry #1: Measure g

Consider a MZI configuration:

Phase shift:

$$\Delta\Phi = N g k_R T_R^2$$

g-Estimator:

$$\hat{g} = \frac{\Delta\Phi}{N k_R T_R^2}$$

Scale factor =
Known to high accuracy

How do we extract knowledge about the spatial variations of g?

Backup: Gradiometry #2: Compare g's

Usual procedure for gradiometry:

$$g(z_0 + \Delta z)$$

$$\Delta g = g(z_0 + \Delta z) - g(z_0)$$

$$g(z_0)$$

Estimator for gravity gradient: $\hat{\Gamma}_0 = \dfrac{\Delta g}{\Delta z}$

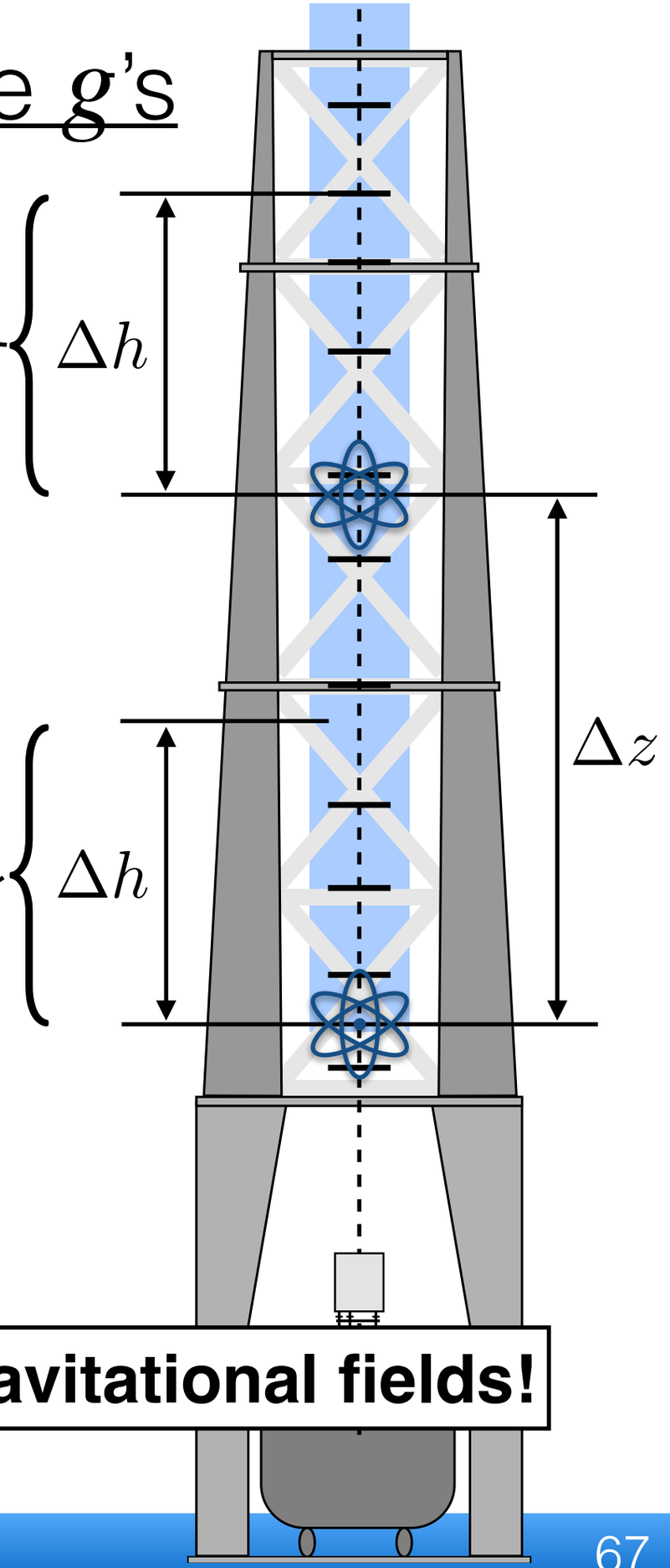

Let us model both in more complicated gravitational fields!

Backup: „Usual“ gradiometry in complex fields

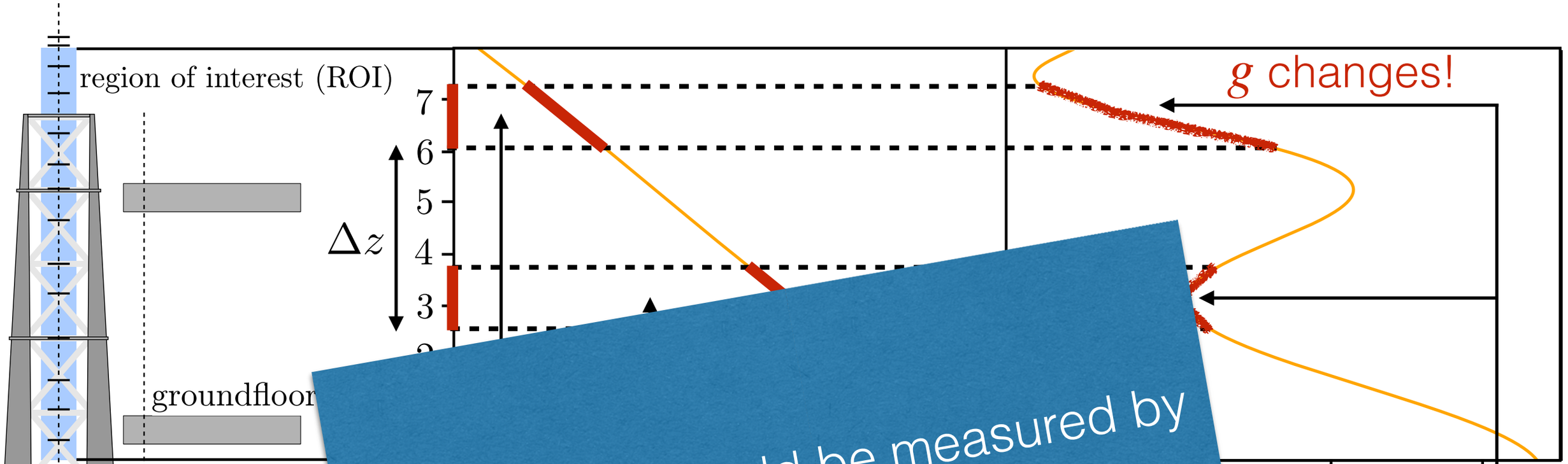

Which signal would be measured by the new CGI?

$$\hat{\Gamma} = \frac{\Delta g}{\Delta z}$$

E… asures „its“ g.

D… ge in g over the height difference.

If you want high spatial resolution

Make Δz and Δh small

Higher measurement uncertainty

Backup: Separation Phase

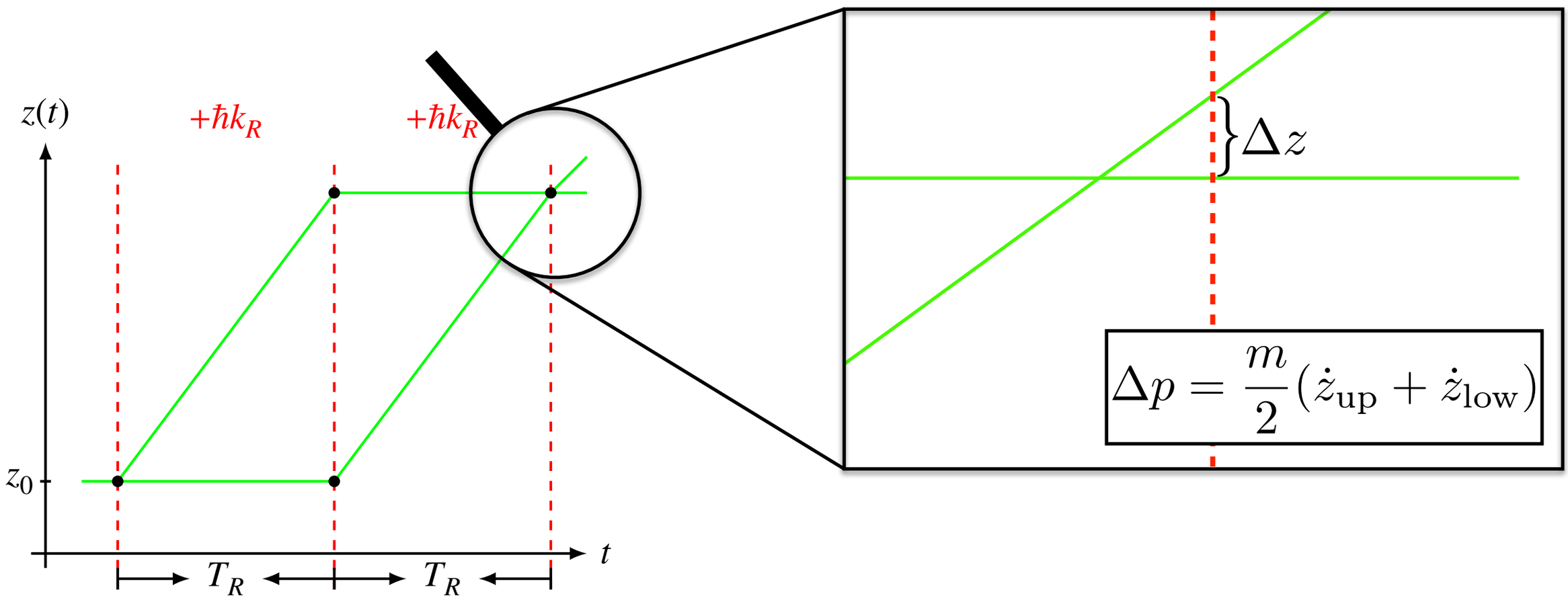

It was shown in REF how one can calculate the phase shift for AIF, which not closes perfectly.

$$\Delta\Phi_{\mathrm{Sep}} = \frac{1}{\hbar}\Delta z \cdot \Delta p$$

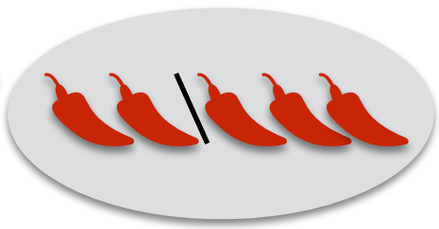

Backup: Python algorithm

We implemented an open source algorithm to calculate the phase shifts of each interferometer very quickly.

```
# ~~~~~~~~~~~~~~~~~~~~~~~~~~~~~~~~~~~~~~~~~~~~~~~~~~~~~~~~~~~~~~~~~~~~~~~~
# ~~ Mach-Zehnder Interferometer (MZI) (3-pulse Interferometer) ~~
# ~~~~~~~~~~~~~~~~~~~~~~~~~~~~~~~~~~~~~~~~~~~~~~~~~~~~~~~~~~~~~~~~~~~~~~~~

interferometer_name = "MZI"
time_decomposition = [0, TR, TR]

bragg_quanta_upper_path = [0, 1, 0, 0]
bloch_quanta_upper_path = [0, 0, 0, 0]
bragg_quanta_lower_path = [0, 0, 1, 0]
bloch_quanta_lower_path = [0, 0, 0, 0]
```

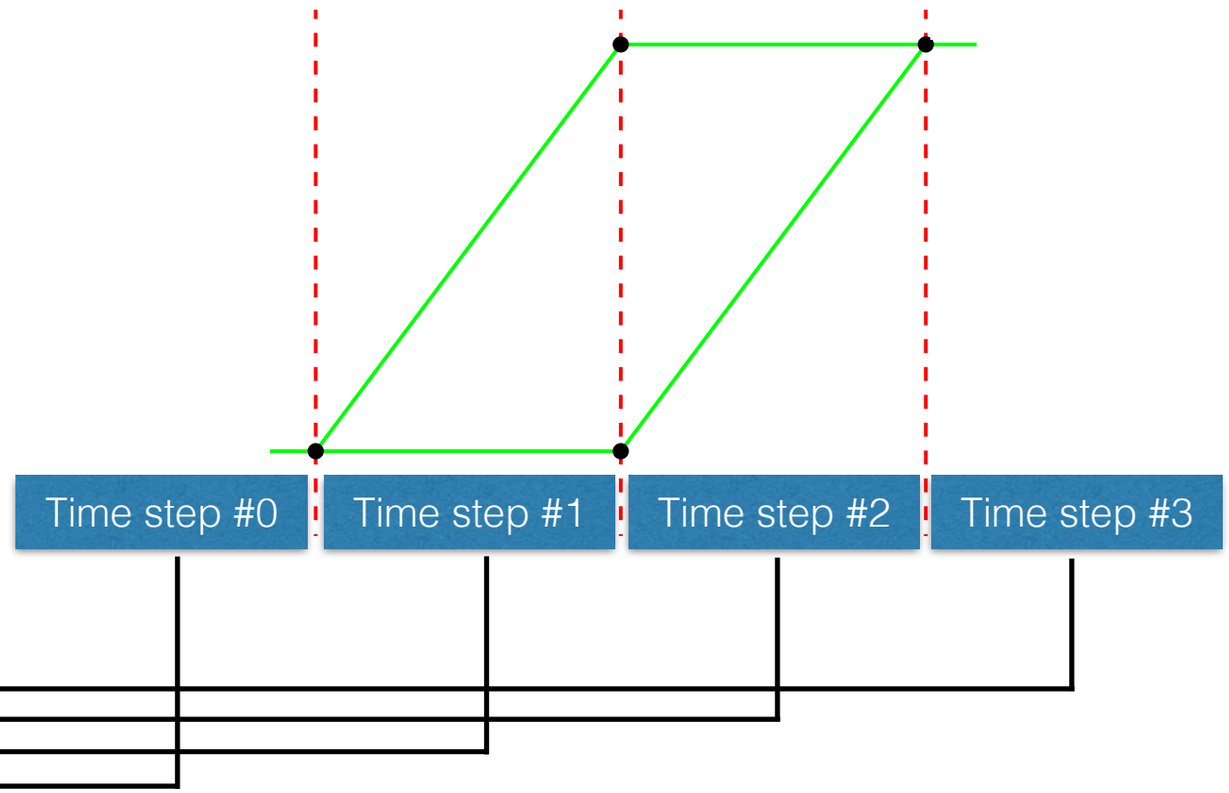

The above initialization is the only thing that has to be done „by hand“. Everything else is automated.

Backup: Dimensionless description

We can use those parameters to rewrite everything dimensionless:

$$z(t) = z_0 + v_0 t - \frac{1}{2} g t^2 + \frac{\Gamma_0}{2} z_0 t^2 + \frac{\Gamma_0}{6} v_0 t^3 + \dots$$

$$\xi = \frac{z}{c T_R}, \quad \tau = \frac{t}{T_R}$$

$$\xi(\tau) = \mathcal{Z}_0 + \mathcal{V}_0 \tau - \frac{1}{2} \mathcal{G}_{1,R} \mathcal{R}_R \tau^2 + \frac{1}{2} \mathcal{G}_{2,R} \mathcal{Z}_0 \tau^2 + \frac{1}{6} \mathcal{G}_{2,R} \mathcal{V}_0 \tau^3 + \dots$$

Using this notation we continue the whole analysis.

Python algorithm

We implemented an open source algorithm to calculate the phase shifts of each AIF very quickly.

The phase shift calculation can quickly become lengthy and prone to errors.

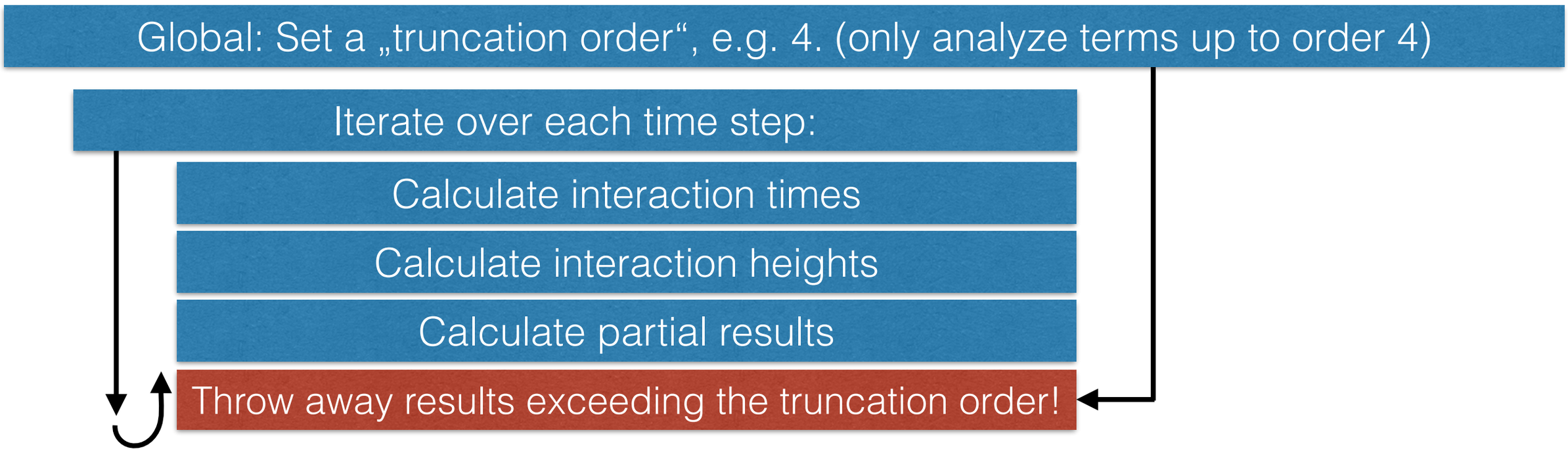

The algorithm truncates dimensionless parameters exceeding a certain number of small parameters. Making the calculation fast and efficient!